



**HAL**  
open science

## Combination of lentiviral and genome editing technologies for the treatment of sickle cell disease

Sophie Ramadier, Anne Chalumeau, Tristan Felix, Nadia Othman, Sherazade Aknoun, Antonio Casini, Giulia Maule, Cecile Masson, Anne de Cian, Giacomo Frati, et al.

### ► To cite this version:

Sophie Ramadier, Anne Chalumeau, Tristan Felix, Nadia Othman, Sherazade Aknoun, et al.. Combination of lentiviral and genome editing technologies for the treatment of sickle cell disease. *Molecular Therapy*, 2022, 30 (1), pp.145-163. 10.1016/j.ymthe.2021.08.019 . hal-03531070

**HAL Id: hal-03531070**

**<https://hal.science/hal-03531070>**

Submitted on 8 Jan 2024

**HAL** is a multi-disciplinary open access archive for the deposit and dissemination of scientific research documents, whether they are published or not. The documents may come from teaching and research institutions in France or abroad, or from public or private research centers.

L'archive ouverte pluridisciplinaire **HAL**, est destinée au dépôt et à la diffusion de documents scientifiques de niveau recherche, publiés ou non, émanant des établissements d'enseignement et de recherche français ou étrangers, des laboratoires publics ou privés.



Distributed under a Creative Commons Attribution - NonCommercial 4.0 International License

# 1 **Combination of lentiviral and genome editing technologies for the treatment of** 2 **sickle cell disease**

3

4 Sophie Ramadier<sup>1,2,3</sup>, Anne Chalumeau<sup>1,2</sup>, Tristan Felix<sup>1,2</sup>, Nadia Othman<sup>3</sup>, Sherazade Aknoun<sup>3</sup>,  
5 Antonio Casini<sup>5</sup>, Giulia Maule<sup>5</sup>, Cecile Masson<sup>6</sup>, Anne De Cian<sup>7</sup>, Giacomo Frati<sup>1,2</sup>, Megane  
6 Brusson<sup>1,2</sup>, Jean-Paul Concordet<sup>7</sup>, Marina Cavazzana<sup>2,8,9</sup>, Anna Cereseto<sup>5</sup>, Wassim El Nemer<sup>10,11,12</sup>,  
7 Mario Amendola<sup>13</sup>, Benoit Wattellier<sup>3</sup>, Vasco Meneghini<sup>1,2,14\*</sup> and Annarita Miccio<sup>1,2\*</sup>

8

9 <sup>1</sup> Laboratory of chromatin and gene regulation during development, Imagine Institute, INSERM UMR1163,  
10 75015, Paris, France

11 <sup>2</sup> Université de Paris, 75015, Paris, France

12 <sup>3</sup> Phasics, Bâtiment Explorer, Espace Technologique, Route de l'Orme des Merisiers, 91190, St Aubin,  
13 France.

14 <sup>5</sup> CIBIO, University of Trento, 38100, Trento, Italy.

15 <sup>6</sup> Paris-Descartes Bioinformatics Platform, Imagine Institute, 75015, Paris, France.

16 <sup>7</sup> INSERM U1154, CNRS UMR7196, Museum National d'Histoire Naturelle, 75015, Paris, France.

17 <sup>8</sup> Imagine Institute, 75015, Paris, France

18 <sup>9</sup> Biotherapy Department and Clinical Investigation Center, Assistance Publique Hopitaux de Paris,  
19 INSERM, 75015 Paris, France

20 <sup>10</sup> Etablissement Français du Sang PACA-Corse, France.

21 <sup>11</sup> Aix Marseille Univ, EFS, CNRS, ADES, 'Biologie des Groupes Sanguins', 13000. Marseille, France.

22 <sup>12</sup> Laboratoire d'Excellence GR-Ex, France.

23 <sup>13</sup> Genethon, INSERM UMR951, 91000, Evry, France

24 <sup>14</sup> Present address: San Raffaele Telethon Institute for Gene Therapy (SR-Tiget), IRCCS San Raffaele  
25 Scientific Institute, 20132, Milan, Italy.

26

27

28

29 \*Correspondence should be addressed to:

30 Annarita Miccio, Imagine Institute, 24 Boulevard du Montparnasse, 75015 Paris, France; e-mail:

31 annarita.miccio@institutimagine.org.

32 Vasco Meneghini, San Raffaele Telethon Institute for Gene Therapy (SR-Tiget), IRCCS San

33 Raffaele Scientific Institute, Via Olgettina 60, 20132, Milano, Italy; e-mail:

34 meneghini.vasco@hsr.it.

35

36

37

38

39

40 **Short title**

41

42 Combining gene addition and editing for SCD

43

44

45

46 **Abstract**

47

48 Sickle cell disease (SCD) is caused by a mutation in the  $\beta$ -globin gene leading to polymerization  
49 of the sickle hemoglobin (HbS) and deformation of red blood cells. Autologous transplantation of  
50 hematopoietic stem/progenitor cells (HSPCs) genetically modified using lentiviral vectors (LVs) to  
51 express an anti-sickling  $\beta$ -globin leads to some clinical benefit in SCD patients, but requires high-  
52 level transgene expression (i.e., high vector copy number [VCN]) to counteract HbS  
53 polymerization.

54 Here, we developed therapeutic approaches combining LV-based gene addition and  
55 CRISPR/Cas9-strategies aimed to either knock-down the sickle  $\beta$ -globin and increase the  
56 incorporation of an anti-sickling globin (AS3) in hemoglobin tetramers, or to induce the expression  
57 of anti-sickling fetal  $\gamma$ -globins. HSPCs from SCD patients were transduced with LVs expressing  
58 AS3 and a guide RNA either targeting the endogenous  $\beta$ -globin gene or regions involved in fetal  
59 hemoglobin silencing. Transfection of transduced cells with Cas9 protein resulted in high editing  
60 efficiency, elevated levels of anti-sickling hemoglobins and rescue of the SCD phenotype at a  
61 significantly lower VCN compared to the conventional LV-based approach.

62 This versatile platform can improve the efficacy of current gene addition approaches, by  
63 combining different therapeutic strategies, thus reducing the vector amount required to achieve a  
64 therapeutic VCN and the associated genotoxicity risk.

65

66

## 67 **Introduction**

68

69  $\beta$ -hemoglobinopathies are severe anemias affecting ~350,000 newborns each year<sup>1</sup>. Sickle cell  
70 disease (SCD) is caused by a point mutation in the sixth codon of the  $\beta$ -globin gene (*HBB*), which  
71 leads to the E6V substitution. Hemoglobin tetramers containing the defective sickle  $\beta^S$ -globin  
72 (HbS) polymerize under hypoxia, and red blood cells (RBCs) assume a sickle shape and become  
73 inflexible. Sickle RBCs have a short half-life and obstruct micro vessels causing a chronic multi-  
74 organ disease associated with poor quality of life and short life expectancy<sup>2</sup>.  $\beta$ -thalassemia is caused  
75 by mutations that reduce or abrogate  $\beta$ -globin production. The uncoupled  $\alpha$ -globin chains cause  
76 apoptosis of erythroid precursors and hemolytic anemia.

77 Current treatments of SCD and  $\beta$ -thalassemia include regular RBC transfusions, which are  
78 associated with significant side effects, such as iron overload and organ damage. The only definitive  
79 cure for  $\beta$ -hemoglobinopathies is the allogeneic hematopoietic stem cell (HSC) transplantation from  
80 HLA-matched sibling donors, which is available only to a fraction of the patients, requires an  
81 immunosuppressive regiment, and can be associated with chronic graft-versus-host disease<sup>3,4</sup>.  
82 Transplantation of autologous HSCs transduced with lentiviral vectors (LVs) carrying an anti-  
83 sickling  $\beta$ -globin transgene (i.e., encoding a  $\beta$ -globin chain inhibiting Hb polymerization) is a  
84 promising therapeutic option for patients lacking a compatible donor<sup>5,6</sup>. In particular, early data  
85 demonstrated a clinical benefit in a SCD patient transplanted with HSCs genetically corrected with  
86 a LV expressing a  $\beta$ -globin chain containing a single anti-sickling amino acid (Q at position 87,  
87 derived from the natural antisickling fetal  $\gamma$ -globin)<sup>7</sup>. However, the analysis of larger cohorts of  
88 patients showed that this treatment is only partially effective in case of poor transgene transfer in  
89 HSCs<sup>8</sup>, which results in therapeutic  $\beta$ -globin levels insufficient to compete with  $\beta^S$ -globin for the  
90 incorporation into the Hb tetramers. Therefore, the achievement of clinically relevant transgene  
91 expression in SCD patients required a high number of integrated LV copies *per* cell, which could  
92 increase the potential genotoxicity risks associated to LV semi-random integration in the

93 genome<sup>9,10</sup>. We have recently optimized a high-titer  $\beta$ -globin-expressing LV (currently used in a  
94 clinical trial for  $\beta$ -thalassemia<sup>11</sup>) for the treatment of SCD by introducing 3 anti-sickling amino  
95 acids substitutions (G16D, E22A, T87Q) in the  $\beta$ -globin chain (AS3)<sup>12</sup>, which prevent the  
96 formation of axial and lateral contacts necessary for the generation of Hb polymers, and increase the  
97 affinity for  $\alpha$ -globin compared to the  $\beta^S$ -globin<sup>6,13</sup>. However, despite these improvements, the RBC  
98 sickling phenotype was only partially corrected even in the presence of a high VCN<sup>6</sup>.

99 Genome editing approaches have been recently developed for the treatment of  $\beta$ -  
100 hemoglobinopathies. Strategies based on the high-fidelity homology-directed repair (HDR) pathway  
101 have been exploited to correct the SCD mutation by providing a DNA donor template containing  
102 the wild-type (WT)  $\beta$ -globin sequence<sup>14-16</sup>. However, the efficiency of HDR-mediated gene  
103 correction is limited in HSCs and gene disruption by non-homologous end joining (NHEJ), a more  
104 active DNA repair pathway in HSCs<sup>17</sup>, may be more frequent, generating a  $\beta$ -thalassemic  
105 phenotype instead of correcting the SCD mutation<sup>18</sup>.

106 The clinical severity of SCD and  $\beta$ -thalassemia is alleviated by the co-inheritance of  
107 mutations causing fetal  $\gamma$ -globin expression in adult RBCs (a condition termed hereditary  
108 persistence of fetal hemoglobin, HbF<sup>19</sup>). The NHEJ pathway has been exploited to induce fetal  $\gamma$ -  
109 globin re-activation by disrupting *cis*-regulatory silencer regions in the  $\gamma$ -globin (*HBG*) promoters<sup>20-</sup>  
110 <sup>23</sup> (e.g., binding sites for BCL11A and LRF transcriptional repressors) and in the  $\beta$ -globin locus<sup>24</sup>,  
111 or to downregulate the BCL11A HbF repressor by targeting its erythroid-specific enhancer<sup>25-27</sup>. The  
112 extent and impact of HbF reactivation on the recovery of SCD and  $\beta$ -thalassemic phenotypes is  
113 currently under investigation in clinical studies<sup>28</sup>.

114 Overall, these pre-clinical and clinical studies show that gene therapy approaches for  $\beta$ -  
115 hemoglobinopathies require highly efficient genetic modification of HSCs and robust expression of  
116 therapeutic globins to achieve clinical benefit.

117 Here, we developed a novel LV platform based on the concomitant expression of the anti-  
118 sickling AS3 transgene and a single guide RNA (sgRNA) targeting the *HBB* gene to induce the

119 downregulation of the endogenous  $\beta^S$  globin in SCD erythroid cells and favor the incorporation of  
120 the therapeutic AS3  $\beta$ -globin chain into Hb tetramers. The versatility of this platform was exploited  
121 by combining the AS3 gene addition with  $\gamma$ -globin re-activation by CRISPR/Cas9-mediated  
122 disruption of the BCL11A binding site in the *HBG* promoters or BCL11A downregulation, thus  
123 potentially extending its application to the treatment of  $\beta$ -thalassemia.

124 Our results demonstrate that editing the *HBB* gene or the *HBG* promoters is safe and  
125 enhances the therapeutic effect of the AS3 gene addition strategy, correcting the SCD pathological  
126 phenotype with a limited number of vector copies per cell.

127

## 128 **Results**

129

### 130 **Selection of an efficient sgRNA downregulating *HBB* expression**

131 To select a sgRNA able to efficiently and safely knock-down the mutant sickle *HBB* gene, we tested  
132 sgRNAs recognizing sequences within the exon 1 of the *HBB* gene (gR-A, gR-B, gR-C, gR-D<sup>29,30</sup>)  
133 (**Fig. 1A**). Plasmids expressing the different sgRNAs under the control of the human U6 promoter  
134 were individually delivered together with a plasmid carrying *SpCas9* nuclease fused with the green  
135 fluorescent protein (Cas9-GFP) in fetal K562 and adult HUDEP-2 erythroid cell lines<sup>31</sup>. The  
136 frequency of insertion and deletions (InDels) ranged from ~40 to ~80% (**Fig. 1B**), as measured by  
137 Sanger sequencing and Tracking of Indels by Decomposition (TIDE) analysis<sup>32</sup>. The frequency of  
138 out-of-frame mutations (likely causing a decreased *HBB* expression) was substantially higher for  
139 gR-C and gR-D (70-95%) than for gR-A and gR-B (25-60%) in both K562 and HUDEP-2 cell lines  
140 (**Fig. 1C**).

141 The ability of the different sgRNAs to downregulate *HBB* expression was evaluated in  
142 HUDEP-2 cells (expressing mainly adult  $\beta$ -globin) differentiated in mature erythroid precursors.  
143 qRT-PCR and western blot analysis showed a strong down-regulation of  $\beta$ -globin expression at

144 both mRNA (70% to 85%) and protein (70% to 90%) levels in comparison to HUDEP-2 cells  
145 transfected only with the Cas9-GFP plasmid (**Fig. 1D, E**). Of note, all the gRNAs generated  
146 premature stop codons (**data not shown**) that likely cause mRNA degradation through nonsense-  
147 mediated decay. As expected from DNA analysis, gR-C and gR-D caused a more robust  $\beta$ -globin  
148 down-regulation compared to gR-A and gR-B (**Fig. 1D, E**). Of note, sgRNAs targeting *HBB* gene  
149 did not alter mRNA expression of the other  $\beta$ -like globin genes (i.e. adult *HBD* and fetal *HBG*  
150 genes; **Fig. 1D**), suggesting a specific targeting of the *HBB* coding sequence. RP-HPLC and CE-  
151 HPLC analyses of differentiated HUDEP-2 cells treated with gR-C showed a decrease in  $\beta$ -globin  
152 production, resulting in an imbalance between  $\alpha$ - and non- $\alpha$  globin chains and accumulation of  $\alpha$ -  
153 globin precipitates, a typical hallmark of  $\beta$ -thalassemia (**Fig. S1A, B**). Notably, the presence of  $\delta$ -  
154 and  $\gamma$ -globin chains was not sufficient to compensate for the lack of  $\beta$ -globin (**Fig. S1A**).

155 The off-target activity of the best performing sgRNAs (gR-C and gR-D) was initially  
156 evaluated in the *HBD* gene, the paralog of the *HBB* gene with the highest sequence homology,  
157 which is often reported as the major off-target locus when targeting the *HBB* gene<sup>33</sup>. gR-C and gR-  
158 D target sequences have 4 and 2 mismatches with the potential off-target locus in *HBD* exon 1 (**Fig.**  
159 **S1C**). TIDE analysis showed absence of InDels in *HBD* in both K562 and HUDEP-2 cells treated  
160 with gR-C or gR-D (**Fig. S1C**). However, plasmid delivery of the CRISPR/Cas9 system in primary  
161 healthy donor (HD) HSPCs resulted in ~3% of edited *HBD* alleles in gR-D-treated cells, while no  
162 off-target events in *HBD* were detected in samples transfected with gR-C (**Fig. S1C**). These  
163 findings are in line with the lower number of mismatches between the gR-D target sequence and the  
164 *HBD* off-target locus as compared to gR-C (**Fig. S1C**). Based on these findings, we further  
165 characterized the off-target activity of gR-C in plasmid-transfected HUDEP-2 cells and primary HD  
166 HSPCs by analyzing the top-15 off-targets predicted by COSMID<sup>34</sup> (**Table S2**). TIDE analysis  
167 revealed no off-target activity in 14 out of 15 loci, including *HBD* and *HBG* genes. InDels were  
168 detected only at the off-target locus 4 (OT4) in HUDEP-2 cells (~2% InDels) and at relatively low

169 levels in primary HSPCs (~0.6% InDels) (**Fig. S1D**). However, this off-target maps to an intergenic  
170 region, which does not contain known hematopoietic *cis*-regulatory regions (**Fig. S1E**).

171 The gR-C was selected for further analyses aimed at evaluating  $\beta$ -globin downregulation in  
172 HSPC-derived erythroid cells, because of its high on-target activity and low off-target editing. We  
173 transfected adult HD HPSCs with plasmids encoding gR-C and Cas9-GFP, and FACS-sorted Cas9-  
174 GFP<sup>+</sup> cells were differentiated towards the erythroid lineage. Genome editing efficiency ranged  
175 between 32% to 54% of InDels with 30 to 49% of out-of-frame mutations in HSPC-derived  
176 erythroid cells (**Fig. 1F; S1F**). We observed  $\beta$ -globin downregulation at both mRNA and protein  
177 levels, which was well correlated with the frequency of frameshift mutations (**Fig. 1F, G, H**). In  
178 HSPC-derived erythroid cells, RP-HPLC analysis revealed that  $\beta$ -globin downregulation induced an  
179 imbalance between the  $\alpha$ - and  $\beta$ -like globin chains, which was not compensated by the presence of  
180  $\gamma$  ( $A\gamma+G\gamma$ )-globin and  $\delta$ -globin chains (**Fig. 1H**). Importantly, CE-HPLC analysis demonstrated that  
181 gR-C led to a substantial reduction of HbA tetramers and accumulation of  $\alpha$ -globin precipitates  
182 (**Fig. 1I**).

183 Overall, these data showed that gR-C is efficient in generating frameshift mutations in *HBB*,  
184 leading to a robust downregulation of  $\beta$ -globin synthesis in both erythroid cell lines and primary  
185 cells.

186

### 187 **A bifunctional lentiviral vector to concomitantly express the AS3 anti-sickling globin and** 188 **down-regulate the endogenous $\beta$ -globin**

189 Transduction of HSPCs isolated from SCD patients with a LV carrying the anti-sickling AS3-globin  
190 transgene (LV AS3) led to a partial correction of SCD phenotype of HSPC-derived RBCs<sup>6</sup>. To  
191 enhance the therapeutic efficacy of gene addition strategies, we introduced a gR-C expression  
192 cassette in LV AS3 to concomitantly induce the expression of the AS3 transgene and the knock-  
193 down of the endogenous  $\beta$ -globin gene upon transient Cas9 delivery, thus favoring the  
194 incorporation of the AS3-globin chain into Hb tetramers. Importantly, the combination of gene

195 addition and gene silencing strategies allows the knock-down of the mutant sickle  $\beta$ -globin gene  
196 only in cells expressing the therapeutic  $\beta$ -globin chain, which will compensate for the reduction of  
197 sickle  $\beta$ -globin chains, thus avoiding the potential generation of a  $\beta$ -thalassemic phenotype.

198 The sgRNA expression cassette was inserted downstream of the AS3-expressing cassette in  
199 reverse orientation to the AS3 transgene transcription (**Fig. 2A**). To further increase gR-C editing  
200 efficiency, we used an optimized sgRNA scaffold carrying a mutation in the RNA pol II  
201 transcription pause sequence and an extended sgRNA duplex to increase U6-driven sgRNA  
202 transcription and sgRNA-Cas9 interactions, respectively<sup>35</sup>. Plasmid transfection of both K562 cells  
203 and adult HD HSPCs showed that the use of the optimized scaffold increased InDel frequency,  
204 while maintaining a similar frequency of out-of-frame mutations (~90%) compared to the original  
205 scaffold (**Fig. S1G, H**). To avoid the downregulation of transgene expression, we introduced six  
206 silent mutations in the AS3 sequence complementary to gR-C (AS3m transgene) using synonymous  
207 codons commonly found in  $\beta$ -like globin genes (**Fig. 2A**). These silent mutations are expected to  
208 impair AS3m targeting and editing by gR-C, which will then recognize only the endogenous  $\beta$ -  
209 globin gene. The insertion of the sgRNA expression cassette did not compromise LV titer ( $\sim 10^9$   
210 TU/ml) and infectivity ( $\sim 7 \cdot 10^4$  TU/ng p24) (LV AS3m.C vector; **Fig. S2A**).

211 To evaluate if the silent mutations impair the production of AS3-chains, we compared LVs  
212 harboring the original (LV AS3) or the modified AS3 transgene (LV AS3m) in a  $\beta$ -thalassemic  
213 HUDEP-2 cell line<sup>36</sup> (HBB KO). In differentiated HBB KO HUDEP-2 cells,  $\beta$ -globin expression is  
214 abolished, resulting in the imbalance between  $\alpha$ - and non  $\alpha$ -chains and accumulation of  $\alpha$ -globin  
215 precipitates (**Fig. S2B, C**). We transduced HBB KO HUDEP-2 cells with LV AS3 and LV AS3m at  
216 increasing multiplicities of infection (MOIs) obtaining a VCN ranging from 0.5 to ~9 (**Fig. S2B,**  
217 **C**). HPLC analyses showed that AS3 expression was comparable in LV AS3- and LV AS3m-  
218 transduced erythroid precursors harboring a similar VCN (**Fig. S2B, C**). Both LVs partially restored  
219 the  $\beta$ -thalassemic phenotype in cells harboring a low VCN (0.5-0.9), while a higher gene marking  
220 (VCN > 4) fully corrected the  $\alpha$ /non- $\alpha$  globin imbalance, as evaluated by RP-HPLC (**Fig. S2B**).

221 These results demonstrated that the silent mutations in the modified transgene do not affect AS3  
222 expression and the production of functional HbAS3 tetramers.

223 To test the capability of LV AS3m.C to downregulate the expression of the endogenous  
224 *HBB* gene, WT HUDEP-2 cells were transduced with increasing doses of LV AS3m.C and then  
225 either transfected with the Cas9-GFP expressing plasmid or mock-transfected. FACS-sorted Cas9-  
226 GFP<sup>+</sup> cells were then differentiated into mature erythroblasts (**Fig. 2B**). The InDel frequency at the  
227 on-target *HBB* gene was positively correlated with the VCN (**Fig. 2C**). *HBB* editing resulted in the  
228 knock-down of the endogenous  $\beta$ -globin at both mRNA and protein levels, with higher InDel  
229 frequency resulting in more robust downregulation of *HBB* expression (**Fig. 2C, D, E**). Of note, no  
230 InDels were detected in the AS3m transgene even in samples displaying a high on-target activity at  
231 the endogenous *HBB* gene, demonstrating that silent mutations in AS3m avoid its targeting by gR-  
232 C, which specifically recognizes the endogenous  $\beta$ -globin gene (**Fig. 2F**). Concordantly, AS3m  
233 mRNA levels were comparable between the control and edited samples (**Fig. 2C**). Importantly, the  
234 downregulation of the endogenous  $\beta$ -globin expression favored the incorporation of AS3 globin  
235 chain into the Hb tetramers (**Fig. 2E**). In cells harboring a relatively low gene marking (VCN of 3  
236 associated with an editing efficiency of 40%), this resulted in a balance between HbA and HbAS3  
237 tetramers, which could not be reached in unedited cells even at high VCN (11.8; **Fig. 2E**). Notably,  
238 the reduction of the  $\beta$ -globin chain content was compensated by the AS3-globin production and  
239 incorporation into the Hb tetramers, thus avoiding the imbalance between the  $\alpha$ - and non- $\alpha$ -chains  
240 and the formation of  $\alpha$ -precipitates (**Fig. 2D, E**). Accordingly, the erythroid differentiation of  
241 HUDEP-2 cells was not impacted by editing of the *HBB* gene as the cell composition was similar in  
242 edited and control HUDEP-2 cells, while HBB KO HUDEP-2 cells showed a delay in  
243 differentiation typical of  $\beta$ -thalassemia<sup>37</sup> (**Fig. S3**).

244 We achieved similar results using a clinically relevant, plasmid-free transfection protocol in  
245 LV-transduced WT HUDEP-2 cells. In particular, we compared Cas9-GFP plasmid or protein  
246 delivery methods in LV AS3m.C-transduced WT HUDEP-2 cells. Transfection with Cas9-GFP

247 protein was less cytotoxic ( $68\pm4\%$  of alive cells in untransfected samples,  $58\pm4\%$  and  $37\pm6\%$  in  
248 samples transfected with 15  $\mu\text{g}$  of Cas9-GFP protein and Cas9-GFP-expressing plasmid,  
249 respectively), more efficient ( $\sim 70\%$  and  $32.5\%$  of GFP<sup>+</sup> cells upon protein and plasmid transfection,  
250 respectively), and led to a higher editing efficiency at the on-target *HBB* locus in unsorted bulk  
251 populations (**Fig. S4A**). LV AS3m.C-transduced WT HUDEP-2 cells transfected with 15  $\mu\text{g}$  of  
252 Cas9-GFP protein were terminally differentiated in mature erythroid precursors. The decrease of  
253 HbA levels and the concomitant increase of HbAS3 content were significantly correlated with the  
254 VCN (**Fig. S4B**) and the genome editing efficiency at the *HBB* locus (**Fig. S4C**). Importantly,  
255 similar amounts of HbA and HbAS3 were detected in cells harboring a VCN of  $\sim 2.5$  and  $\sim 46\%$  of  
256 edited alleles (**Fig. S4B, C**). On the contrary, in mock-transfected LV AS3m.C-transduced cells,  
257 HbA content exceeded the levels of HbAS3 even in cells harboring a high VCN (**Fig. S4B**).

258 Overall, these data showed that the treatment with LV AS3m.C can safely and efficiently  
259 down-regulate the expression of the endogenous  $\beta$ -globin and increase the production of Hb  
260 tetramers containing the therapeutic AS3-globin compared to the classical gene addition approach.

261

## 262 **A bifunctional lentiviral vector to induce the expression of the anti-sickling AS3-globin and $\gamma$ -** 263 **globin chains**

264 Considering the therapeutic benefit of high fetal  $\gamma$ -globin expression in SCD and  $\beta$ -thalassemia  
265 patients<sup>38-40</sup>, we exploited the flexibility of this novel LV platform to simultaneously express the  
266 AS3m transgene and reactivate HbF expression. The combined expression of AS3- and  $\gamma$ -chains can  
267 elevate the total Hb content in  $\beta$ -thalassemia patients and, as both these globins display anti-sickling  
268 properties, it can also benefit SCD patients.

269 We generated LVs expressing the AS3m transgene and a sgRNA that either disrupts a  
270 sequence in the *BCL11A* erythroid-specific enhancer critical for its expression (AS3m.BCL11A)<sup>26</sup>  
271 or generates 13-bp deletions encompassing the BCL11A binding site in the fetal  $\gamma$ -globin promoters

272 (AS3m.13bpdel)<sup>20</sup> (**Fig. 2A**). As observed for LV AS3m.C, the insertion of the sgRNA cassette did  
273 not impair LV titer and infectivity (**Fig. S2A**).

274 WT HUDEP-2 cells were transduced with LV AS3m.BCL11A or LV AS3m.13bpdel, and  
275 then transfected with Cas9-GFP plasmid or mock-transfected. FACS-sorted Cas9-GFP<sup>+</sup> cells and  
276 control samples were differentiated in mature erythroid precursors (**Fig. 2B**). Editing of the  
277 *BCL11A* enhancer or the  $\gamma$ -globin promoters did not impact the differentiation of HUDEP-2 cells  
278 (**Fig. S3**). LV AS3m.BCL11A-transduced cells showed up to 63% of InDel frequency at the  
279 *BCL11A* enhancer, which caused a strong decrease in the levels of *BCL11A-XL*, the isoform mainly  
280 involved in the inhibition of HbF expression<sup>41,42</sup> (**Fig. S5A**). In LV AS3m.13bpdel-transduced cells,  
281 around one third ( $31.7 \pm 0.5\%$ ) of the total editing events generated by gR-13bpdel were MMEJ-  
282 mediated 13-bp deletions removing the entire BCL11A binding site (**Fig. S5B**). All other events  
283 also led to the disruption of the BCL11A binding site in the *HBG* promoters (**Fig. S5B**). Editing of  
284 the BCL11A enhancer or the  $\gamma$ -globin promoters resulted in *HBG* gene induction, and increased  $\gamma$ -  
285 globin chain and HbF production (**Fig. 2G, H, I**). In particular, the concomitant expression of AS3  
286 and  $\gamma$ -globin resulted in up to 37% and 55% of total anti-sickling hemoglobins (HbF+HbAS3) in  
287 LV AS3m.BCL11A- and LV AS3m.13bpdel-transduced cells, respectively (**Fig. 2I**). The combined  
288 expression of HbF and HbAS3 decreased adult HbA production in samples with the higher genome  
289 editing frequencies (**Fig. 2I**). Flow cytometry analysis confirmed the increased HbF production with  
290 up to 61% and 74% of F-cells in samples treated with LV AS3m.BCL11A and LV AS3m.13bpdel,  
291 respectively (**Fig. S5C**).

292 These data show that CRISPR/Cas9-mediated induction of HbF expression can increase the  
293 total Hb content in cells expressing a  $\beta$ -globin therapeutic transgene, thus representing a promising  
294 strategy to correct both SCD and  $\beta$ -thalassemia phenotypes.

295

296 **The combination of gene addition and genome editing approaches increased the content of**  
297 **anti-sickling hemoglobins in SCD RBCs**

298 The efficacy and safety of our approach was evaluated in adult plerixafor-mobilized peripheral  
299 blood (mPB) HSPCs from SCD patients. HSPCs were transduced with increasing doses of LV  
300 AS3m.C and transfected 48 hours later with Cas9-GFP protein using previously optimized  
301 protocols<sup>6,43</sup> (**Fig. 3A**). Control and edited SCD HSPCs were plated in clonogenic cultures (colony  
302 forming cell [CFC] assay) allowing the growth of erythroid (BFU-E, burst-forming unit-erythroid)  
303 and granulomonocytic (CFU-GM, colony-forming unit granulocyte-macrophages) progenitors. The  
304 electroporation of transduced cells modestly reduced the number of progenitors, although this  
305 decrease was not statistically significant (**Fig. S6A**). Importantly, no significant difference was  
306 observed between LV AS3m.C-transduced, mock-transfected and edited samples (**Fig. S6A**). Upon  
307 differentiation in mature erythroblasts, we observed a significant correlation between editing  
308 efficiency at the *HBB* locus and VCN, with an InDel frequency ranging from 21% to 67% (**Fig.**  
309 **3B**). A positive correlation between editing frequency and VCN was also observed in pools of  
310 BFU-E derived from SCD HSPCs treated with LV AS3m.C and Cas9-GFP protein (**Fig. S6B**). As  
311 previously observed in HUDEP-2 cells, no InDels were detected in the sequence of the AS3m  
312 transgene in any of the treated samples (**Fig. 3C**). Deep sequencing analysis in edited erythroblasts  
313 revealed a low off-target activity only in 1 out of the 4 off-target sites detected by genome-wide  
314 GUIDE-seq analysis (**Fig. 3D**). This locus corresponds to the OT4 previously identified in primary  
315 HSPCs by Sanger sequencing (**Fig. S1D, E**).

316 Erythroblasts were further differentiated in enucleated RBCs using a 3-phase protocol<sup>44</sup>  
317 (**Fig. 3A**). We observed a positive correlation between VCN and the HbAS3 content in RBCs  
318 derived from mock-transfected, LV AS3m.C-transduced HSPCs achieving equivalent HbS and  
319 HbAS3 levels at a VCN of ~5.5 (**Fig. 3E**). Cas9 treatment led to a decreased expression of the  
320 sickle *HBB* gene at both mRNA and protein levels, thus, favoring the incorporation of the AS3  
321 chain in Hb tetramers (**Fig. 3E-F and Fig. S6C**). Importantly, in RBCs derived from edited SCD  
322 HSPCs, similar amounts of HbS and HbAS3 were observed already at a VCN of ~2.2 (InDel  
323 frequency of ~41%), reproducing the Hb profile of asymptomatic SCD carriers (**Fig. 3E**). HbS

324 down-regulation and increased incorporation of the AS3 chain in Hb tetramers were still evident at  
325 low VCN (**Fig. 3E-F and Fig. S6C**) Notably, CE-HPLC showed absence of  $\alpha$ -globin precipitates in  
326 RBCs obtained from edited HSPCs indicating that the expression of the AS3 chain was able to  
327 efficiently compensate for the lack of  $\beta$ s-globin expression and avoid the generation of a  $\beta$ -  
328 thalassemic phenotype (**Fig. 3G**).

329 In parallel, SCD mPB HSPCs were transduced with increasing doses of LV AS3m.13bpdel  
330 transfected with Cas9-GFP protein and then differentiated towards the erythroid lineage (**Fig. 4A**).  
331 No significant differences were observed in the number of BFU-E and CFU-GM between control  
332 and edited samples (**Fig. S6A**). We observed a direct correlation between VCN and InDel frequency  
333 in BFU-Es and mature erythroblasts (**Fig. 4B and Fig. S6B**). LV AS3m.13bpdel-transduced  
334 erythroblasts showed ~30% of edited loci at a VCN of 3-4, and up to 50% at higher VCNs (**Fig. 4B**  
335 **and Fig. S6B**). On the contrary, SCD mPB HSPCs transduced with LV AS3m.BCL11A were  
336 poorly edited, reaching a maximum of ~20% of InDel efficiency (**Fig. 4B**). Deep-sequencing  
337 analyses of the only gR-13bpdel off-target previously detected by GUIDE-seq<sup>23</sup> revealed no off-  
338 target activity in LV AS3m.13bpdel-transduced erythroblasts (**Fig. 4C**). GUIDE-seq analysis in  
339 293T cells showed a high number of off-target sites for the sgRNA targeting the *BCL11A* enhancer  
340 (**Fig. 4D**).

341 Given the low efficiency of LV AS3m.BCL11A and the high number of off-target sites, we  
342 further differentiated into enucleated RBCs only the cells derived from edited, LV AS3m.13bpdel-  
343 transduced HSPCs to evaluate the content of anti-sickling globins. The treatment of LV  
344 AS3m.13bpdel-transduced SCD HSPCs with Cas9-GFP protein led to an increased *HBG* mRNA  
345 expression (**Fig. 4E**), reaching a percentage of F-cells ranging from 40% to 85% (**Fig. 4F**). CE-  
346 HPLC analysis showed that the total amount of anti-sickling hemoglobins (HbF+HbAS3) was  
347 positively correlated with the VCN and the editing frequency (**Fig. 4G-H**). The concomitant AS3-  
348 globin chain expression and  $\gamma$ -globin reactivation resulted in reduced HbS levels (**Fig. 4G-H**).  
349 Importantly, similar amounts of HbS and anti-sickling hemoglobins were obtained at a lower VCN

350 (VCN of ~3.7; 34% of InDels) in edited cells compared to the mock-transfected samples (VCN of  
351 ~5.4) (**Fig. 4 G-H**). Importantly,  $\gamma$ -globin reactivation was still observed in edited samples at low  
352 VCN (**Fig. 4G-H** and **Fig. S6D**)

353

#### 354 **The increased content of anti-sickling hemoglobins rescues the SCD cell phenotype**

355 To assess the effect of the increased production of anti-sickling Hb tetramers on RBC sickling, we  
356 performed a deoxygenation assay to measure the proportion of sickle-shaped RBCs. *In vitro*  
357 generated RBCs were exposed to an oxygen-deprived atmosphere, which induces HbS  
358 polymerization and RBC sickling. The percentage of sickled cells was decreased in RBC  
359 populations derived from mock-transfected, LV AS3m.C- and AS3m.13bpdel-transduced HSPCs  
360 compared to untreated SCD controls as a consequence of the expression of the AS3-globin chain,  
361 with 40 to 60% of normal, doughnut-shaped RBCs at a VCN of ~2 to 3 (**Fig. 5**). Interestingly, in  
362 RBCs derived from edited LV AS3m.C-transduced HSPCs, HbS downregulation combined with the  
363 high HbAS3 expression resulted in a substantial increase in the proportion of corrected RBCs (**Fig.**  
364 **5**). This effect was still evident by comparing RBCs generated from edited and mock-transfected  
365 LV AS3m.C-transduced HSPCs with a higher VCN (**Fig. 5**). Finally, the increased HbF amount  
366 induced by the editing of the *HBG* promoters led to a modest but still significant reduction in the  
367 percentage of sickle-shaped RBCs compared to samples obtained from unedited, LV  
368 AS3m.13bpdel-transduced HSPCs showing a similar VCN (**Fig. 5**).

369

#### 370 **Erythroid cell differentiation and red blood cell properties remain largely unchanged upon** 371 **editing of SCD HSPCs**

372 To exclude any impairment in erythroid differentiation of edited HSPCs, we monitored over time  
373 the erythroid liquid cultures using flow cytometry and quantitative phase imaging. In particular,  
374 although the co-expression of the AS3-globin and the sgRNA targeting *HBB* should avoid the  
375 excessive reduction of  $\beta$ -like globin chains, a potential issue of this strategy is the possibility to

376 generate a  $\beta$ -thalassemic phenotype in the absence of a sufficient amount of transgene-derived AS3-  
377 globin to compensate  $\beta^S$ -downregulation.

378 SCD HSPCs were transduced with the LV AS3m.C, transfected with Cas9-GFP protein, and  
379 then *in vitro* differentiated into mature RBCs (**Fig. 6A**). Erythroid cultures obtained from SCD or  
380 HD HSPCs transfected with Cas9 ribonucleoprotein (RNP) complexes containing gR-C were used  
381 as  $\beta$ -thalassemia-like control cells (**Fig. 6A**). Mature RBCs derived from SCD or HD HSPCs  
382 treated with gR-C-RNP displayed a strong reduction in the HbS and HbA content, respectively, and  
383 an increased  $\alpha$ -/non  $\alpha$ -chain ratio in comparison to untreated controls (**Fig. 6B**). On the contrary, in  
384 RBCs derived from *HBB*-edited, LV AS3m.C-transduced SCD HSPCs,  $\alpha$ -/non- $\alpha$ -chain ratios  
385 remained largely unchanged ( $1.08 \pm 0.04$ ; n=14) compared to untreated controls and mock-  
386 transfected, LV AS3m.C-treated samples ( $1.05 \pm 0.03$  n=15)

387 The erythroid differentiation of edited HSPCs cells treated with LV AS3m.C was not  
388 impaired. Indeed, the expression of surface markers identifying the different erythroid populations  
389 (CD36, CD71, CD235A, CD49d and Band3) and the frequency of enucleated cells were similar in  
390 control and treated samples all along the differentiation (**Fig. 7A-E, S7A**). On the contrary, in  $\beta$ -  
391 thalassemia-like cells erythroid differentiation was delayed as well as RBC enucleation (**Fig. 7A-E**).

392 Furthermore, we acquired images from *in vitro* differentiated RBCs derived from SCD  
393 HSPCs treated with LV AS3m.C to evaluate several morphological and physical parameters in a  
394 quantitative manner (**Fig. 6A**).  $\beta$ -thalassemia-like RBCs were characterized by a reduced dry mass  
395 compared to mock-treated control samples, due to the lower Hb content (**Fig. 7F, S7B**). Surface,  
396 perimeter and ellipticity parameters were altered in  $\beta$ -thalassemia-like RBCs (**Fig. 7G-I, S7C-E**),  
397 reflecting the anisocytosis and poikilocytosis characterizing  $\beta$ -thalassemic RBCs<sup>45,46</sup>. In RBCs  
398 derived from LV AS3m.C-treated SCD HSPCs harboring ~42% of edited *HBB* alleles, only a small  
399 percentage of cells showed reduced dry mass, surface, and perimeter ( $6.2 \pm 2.3\%$ ,  $5.4 \pm 3.6\%$  and  
400  $6.5 \pm 3.7\%$ ; n=2, respectively) in comparison to RBCs obtained from mock-transfected LV AS3m.C  
401 HSPCs (**Fig. 7F-H, S7B-D**), while ellipticity was overall unaffected (**Fig. 7I, S7E**). These

402 frequencies were modestly increased in RBCs derived from SCD HSPCs harboring 63% of edited  
403 alleles (10.1% for dry mass, 13.4% for surface and 10.2% for perimeter).

404 Finally, editing of *HBG* promoters did not impact the differentiation and enucleation of LV  
405 AS3m.13bpdel-transduced SCD HSPCs (**Fig. S8B-E**). Alpha-/non- $\alpha$ -chain ratios, surface, dry mass,  
406 perimeter and ellipticity were similar in RBCs derived from edited LV AS3m.13bpdel-transduced  
407 HSPCs and control samples (**Fig. S8A, S8F-I**).

408 In conclusion, these analyses showed that erythroid differentiation of SCD HSPCs edited  
409 using bifunctional LVs and cas9 transfection is largely unaltered.

410

## 411 Discussion

412

413 LVs expressing a  $\beta$ -globin transgene to compensate  $\beta$ -globin deficiency in  $\beta$ -thalassemia, or to  
414 inhibit Hb polymerization in SCD have shown promising clinical outcomes<sup>7,11,47</sup>. However, to be  
415 effective, gene addition strategies require the sustained engraftment of highly transduced HSCs<sup>48</sup>.  
416 This could increase the genotoxic risk particularly in SCD patients who have an increased  
417 probability of developing hematological malignancies compared to the general population<sup>49,50</sup>.  
418 While promising approaches aimed at improving LV-derived transgene expression have been  
419 investigated<sup>51</sup>, reaching therapeutic globin expression with a low VCN is still challenging as LVs  
420 cannot accommodate the entire  $\beta$ -globin locus control region ( $\beta$ LCR) responsible for high-level  
421 expression of the  $\beta$ -like globin genes.

422 Interestingly, clinical observations in a compound  $\beta^0/\beta^S$  heterozygous SCD patient indicate  
423 that  $\beta$ -globin deficiency was associated with amelioration of the disease phenotype despite the  
424 relatively low gene marking in engrafted HSCs<sup>8</sup>. Furthermore, a mild disease phenotype is observed  
425 in SCD and  $\beta$ -thalassemia patients harboring HPFH mutations<sup>19,52,53</sup>. These clinical observations  
426 support the rationale of the design of gene therapy approaches that combine the expression of an  
427 anti-sickling  $\beta$ -globin transgene with editing strategies aimed to either reduce the  $\beta^S$ -globin

428 expression or to increase the  $\gamma$ -globin content to counteract HbS polymerization in SCD or to  
429 increase Hb content in  $\beta$ -thalassemia.

430 We designed LVs simultaneously driving the expression of a  $\beta$ -globin chain carrying three  
431 anti-sickling amino acids<sup>13</sup>, and a sgRNA either to introduce frameshift mutations in the *HBB* gene  
432 (LV AS3m.C), or to reactivate HbF expression by disrupting the BCL11A binding site in the  $\gamma$ -  
433 globin promoters (LV AS3m.13bpdel)<sup>5</sup> or by downregulating BCL11A expression (LV  
434 AS3m.BCL11A)<sup>5</sup>.

435 The editing efficiency at the on-target loci was positively correlated with the number of  
436 integrated LV copies in HUDEP-2 cells and SCD primary HSPCs, demonstrating the efficient LV-  
437 derived sgRNA expression and the formation of the functional CRISPR/Cas9 RNP complexes in  
438 transfected cells. These data are in line with combinatorial systems based on the stable LV-  
439 mediated delivery of sgRNAs coupled with transient transfection of Cas9 mRNA in human HD  
440 HSPCs to downregulate the expression of cell surface proteins<sup>54</sup>. Importantly, we achieved high  
441 editing efficiencies using Cas9 protein delivery that we previously demonstrated to be less toxic and  
442 more efficient than mRNA delivery in primary HSPCs<sup>43</sup>. A recent report showed that  
443 precomplexing of Cas9 protein with a non-targeting sgRNA was required to achieve high genome  
444 editing frequency using LV-delivered sgRNAs<sup>55</sup>. Interestingly, our system was already efficient by  
445 transfecting Cas9 protein alone and the editing efficiency was not further increased by complexing  
446 the Cas9 with a nontargeting sgRNA (**data not shown**). Importantly, we applied this technology to  
447 develop a gene therapy approach for  $\beta$ -hemoglobinopathies by combining the efficient LV-based  
448 delivery of sgRNAs with the expression of a therapeutic  $\beta$ -globin transgene.

449 The delivery of Cas9 protein in clinically relevant SCD HSPCs transduced with LV AS3m.C  
450 resulted in robust downregulation of *HBB* expression at both mRNA and protein levels. On the  
451 contrary, introduction of silent mutations in the AS3 sequence prevented undesired editing and  
452 inactivation of the transgene. The increased availability of  $\alpha$ -globin chains caused by  $\beta$ -globin  
453 downregulation favored the formation of AS3-containing Hb tetramers, thus increasing the total

454 anti-sickling Hb content in RBCs derived from edited HSPCs, as compared to RBCs obtained from  
455 control HSPCs harboring a similar number of LV copies. In a parallel approach, the editing of the  $\gamma$ -  
456 globin promoters in SCD HSPCs transduced with LV AS3m.13bpdel increased the total content of  
457 anti-sickling Hb tetramers by inducing the expression of both G $\gamma$ - and A $\gamma$ -globins. As previously  
458 reported<sup>20,23,56,57</sup>, editing of the -115 region of the *HBG* promoters disrupts the *BCL11A* binding  
459 site and evicts BCL11A, allowing the recruitment of the NF-Y transcriptional activator at the -86  
460 region and  $\gamma$ -globin reactivation. The sgRNAs targeting *HBB* gene or the *HBG* promoters showed  
461 minimal off-target activity as detected by GUIDE-seq and targeted NGS sequencing of the potential  
462 off-targets. However, although GUIDE-seq was identified as the best-performing assay for *ex vivo*  
463 therapeutics<sup>58-60</sup>, it has a limited sensitivity (0.1%) and therefore could fail to detect off-target  
464 events that occur at a low frequency but can still potentially lead to deleterious outcomes (e.g.,  
465 clonal expansion and malignant neoplasms). More sensitive assays to assess the potential  
466 CRISPR/Cas9-associated genotoxic risk should be developed in particular for clinical applications  
467 aimed to modify hundreds of millions of cells.

468 Surprisingly, LV AS3m.BCL11A showed poor transduction and editing efficiencies in the  
469 *BCL11A* erythroid-specific enhancer in SCD HSPCs. We have not clarified the mechanisms of poor  
470 transduction by LV AS3m.BCL11A. In cell lines, we have not observed any significant difference  
471 in titer and infectivity between LV AS3m.BCL11A and the other vectors, although the LV  
472 harboring the gRNA targeting the *BCL11A* enhancer tends to have a lower infectivity that could  
473 impact the efficiency of transduction of primary HSPCs. In our previous study, we also compared  
474 LVs with similar titer and infectivity (as determined in cell lines) and observed, for some of these  
475 vectors, a low transduction of HSPCs, likely related to specific sequences that are detrimental to the  
476 vector performance in primary cells<sup>43</sup>. Furthermore, bi-allelic disruption of this enhancer is required  
477 to achieve HbF reactivation and the selected sgRNA targeting *BCL11A*<sup>26</sup> showed numerous  
478 potential off-target sites. For these reasons, we decided to not further pursue this approach. The

479 selection of a more efficient and specific sgRNA disrupting critical regions in the *BCL11A* enhancer  
480 will allow us to ameliorate this therapeutic approach in future experiments.

481 Interestingly, the high content of anti-sickling hemoglobins observed with both LV AS3m.C  
482 and LV AS3m.13bpdel resulted in reduced HbS levels, Hb polymerization and frequency of sickled  
483 RBCs compared to the conventional gene addition approach. Importantly, compared to a LV  
484 expressing only the anti-sickling transgene, our combined approach requires a lower VCN to  
485 achieve a therapeutic effect, thus reducing the potential genotoxicity risk associated to LV  
486 integration. In particular, we achieved similar amounts of HbS and anti-sickling hemoglobins  
487 (resembling the Hb profile of an asymptomatic heterozygous SCD carrier) with a VCN of ~5.5  
488 using the conventional gene addition strategy, and a VCN of ~2.2 and ~3.7 (associated with 30-35%  
489 of edited *HBB* or *HBG* genes) using LV AS3m.C and LV AS3m.13bpdel, respectively. As a higher  
490 VCN was required to reach a similar editing frequency for LV AS3m.13bpdel compared to LV  
491 AS3m.C, we hypothesize that the difference in the extent of the correction of the disease phenotype  
492 between these two approaches is due to the higher editing efficiency of the gR-C compared to the  
493 sgRNA targeting the *HBG* promoters. Alternative sgRNAs targeting HbF inhibitory sequences<sup>23,61</sup>  
494 could be tested in future studies to further enhance  $\gamma$ -globin reactivation with a lower VCN.

495 Importantly, we used flow cytometry and quantitative phase imaging to evaluate erythroid  
496 differentiation of edited HSPCs and quantify at single cell level morphological and physical  
497 parameters of *in vitro* differentiated RBCs. This study is fundamental to demonstrate the safety of  
498 HSC-based treatments for  $\beta$ -hemoglobinopathies.  $\beta$ -thalassemic erythroid cells showed delayed  
499 differentiation and enucleation, imbalance in the  $\alpha$ -/non  $\alpha$ -chain ratio,  $\alpha$ -precipitates, anisocytosis  
500 and poikilocytosis. Editing of the *HBB* gene or the  $\gamma$ -globin promoters in HSPCs did not negatively  
501 impact their differentiation and enucleation rate, allowing the production of mature RBCs with Hb  
502 content and morphological parameters largely similar to untreated controls. In particular, in  
503 erythroid cells derived from *HBB*-edited HSPCs, AS3-globin chain expression was sufficient to  
504 compensate for the lack of  $\beta^s$ -globin expression in the vast majority of RBCs. In fact, only a small

505 percentage of RBCs (~5 to 10%) displayed a  $\beta$ -thalassemic-like phenotype. We can speculate that a  
506 small fraction of poorly transduced HSPCs harboring bi-allelic disruption of *HBB* gene give rise to  
507 this RBC subpopulation producing AS3 levels, which are insufficient to compensate  $\beta^S$ -  
508 downregulation. Importantly, preclinical and clinical data indicate that in allotransplanted or gene  
509 therapy treated  $\beta$ -thalassemia subjects,  $\beta$ -thalassemic cells are counter selected *in vivo* because the  
510 erythroid precursors undergo apoptosis, and mature RBCs have a shorter lifespan compared to HD  
511 or corrected cells<sup>5,11,62</sup>. Furthermore, we do not expect that such a low frequency of  $\beta$ -thalassemic  
512 RBCs will impact the correction of SCD phenotype *in vivo*.

513 Other therapeutic strategies for SCD aim at reverting the SCD mutation by cleaving the  
514 sickle *HBB* gene using the CRISPR/Cas9 system and inserting through the HDR pathway a donor  
515 template containing the WT *HBB* sequence that is either provided as single strand oligonucleotide  
516 or delivered by a viral vector<sup>14,63,64</sup>. More recently, we proposed a combined treatment for  $\beta$ -  
517 thalassemia based on the insertion of the AS3 transgene in the  $\alpha$ -globin (*HBA*) locus to  
518 simultaneously express the therapeutic  $\beta$ -globin while reducing *HBA* expression levels<sup>36</sup> and  $\alpha$ -  
519 globin precipitates. However, although more promising than the standard gene addition strategy,  
520 these approaches currently suffer from poor HDR efficiency in HSCs. On the contrary, our  
521 combined approach is likely more prone to produce the desired genome modification as it relies on  
522 the NHEJ pathway, known to be preferentially active and more efficient in HSCs compared to  
523 HDR<sup>65-68</sup>. Moreover, in SCD, failed HDR-mediated gene correction likely results in the NHEJ-  
524 mediated *HBB* gene disruption, which could likely not be compensated by the residual endogenous  
525  $\beta$ -like globin chains, thus potentially generating a  $\beta$ -thalassemic phenotype<sup>69</sup>. On the contrary,  
526 generation of a  $\beta$ -thalassemia phenotype was observed only in a small fraction of RBCs using our  
527 combined strategy as the same LV is co-expressing the sgRNA targeting *HBB* and the therapeutic  
528 AS3 chain that compensates for the knock-down of the endogenous *HBB*.

529 Ongoing trials for  $\beta$ -hemoglobinopathies using a genome editing strategy efficiently  
530 targeting the *BCL11A* enhancer showed early promising results<sup>28</sup>. However, HbF reactivation and

531 therapeutic benefit were modest when editing occurred at low efficiency<sup>40</sup>. Furthermore, as reported  
532 in trials based on LV gene addition approaches, some patients did not attain normal levels of total  
533 Hb, and in SCD subjects HbS levels were not always decreased to the values observed in  
534 asymptomatic heterozygous SCD carrier, suggesting the persistence of a subset of non-corrected  
535 RBCs<sup>70</sup>.

536 Our strategies combine two gene therapy platforms currently under evaluation in  
537 experimental clinical trials for  $\beta$ -hemoglobinopathies, potentially improving the efficacy of gene  
538 therapy to treat SCD and even  $\beta$ -thalassemia when AS3 expression is combined with HbF re-  
539 activation. Notably, in our strategies bi-allelic editing is likely not required when targeting either the  
540 sickle  $\beta$ -globin gene or the *HBG* promoters. However, there are some concerns related to the risks  
541 of combining LV and CRISPR/Cas9 approaches, which can both lead to potential deleterious DNA  
542 mutagenesis and DNA damage response. Despite our study suggests that the treatment of patient  
543 HSPCs with both LV and Cas9 did not affect progenitor growth and differentiation, predictive  
544 assays, such as xenotransplantation in immunodeficient mouse models, are required to demonstrate  
545 the safety of the proposed approaches in repopulating stem cells and their progeny.

546 Finally, bifunctional LVs can have a wider range of potential applications in this field. In  
547 fact, by simply modifying the sgRNA sequence, the bifunctional LVs could be exploited to develop  
548 different therapeutic approaches for  $\beta$ -hemoglobinopathies (e.g., sickle  $\beta$ -globin or *BCL11A* down-  
549 regulation<sup>26</sup>; inactivation of *HBG* inhibitory sequences<sup>20,23</sup>; insertion of *HBG* activating  
550 sequences<sup>71,72</sup>) by using a variety of editing tools (e.g., Cas9 nucleases, base editors, epigenome  
551 editors and prime editors<sup>73-75</sup>).

552 More generally, the combination of gene addition and genome editing strategies has the  
553 potential to simultaneously induce the expression of therapeutic proteins and downregulate disease-  
554 causing genes. By way of example, we envision that this versatile technology can allow the  
555 development of therapeutic strategies for the treatment of autosomal dominant disorders, which  
556 requires the down-regulation of the dominant allele. As it is difficult to achieve targeted

557 downregulation of the mutant gene without impairing the expression of the WT allele, our strategy  
558 could allow the disruption of the endogenous genes, and simultaneously the LV-derived expression  
559 of a non-targeted WT allele (i.e. harboring silent mutations, which impair sgRNA binding and  
560 transgene disruption).

561

562

## 563 **Materials and Methods**

564

### 565 **Lentiviral vector production and titration**

566 For LV production, the expression cassette consisting of DNase I hypersensitive sites HS2  
567 (genomic coordinates [hg38]: chr11:5280255-5281665) and HS3 (genomic coordinates [hg38]:  
568 chr11:5284251-5285452) of the  $\beta$ LCR<sup>76</sup>, and a *HBB* mini-gene extending from -265 bp upstream of  
569 the transcriptional start site to +300 bp downstream of the poly(A)-addition site (genomic  
570 coordinates[hg38]: chr11:5225174-5227336) with a short version of intron 2 (genomic  
571 coordinates[hg38]: chr11:5203703-5204295) was cloned into a pCCL lentiviral vector backbone to  
572 generate the pCCL. $\beta$ -globin plasmid. The mutations determining three anti-sickling amino acid  
573 substitutions (G16D, E22A and T87Q)<sup>13</sup> were introduced in the pCCL. $\beta$ -globin plasmid by *in vitro*  
574 site-directed mutagenesis to obtain the pCCL.AS3 plasmid. Silent mutations were inserted in the  
575 19-bp AS3 transgene sequence recognized by gR-C to generate the pCCL.AS3m plasmid. To insert  
576 silent mutations, we used synonymous codons from *HBB*, *HBD*, *HBG1* and *HBG2* genes.

577 Synthetic oligonucleotides (Integrated DNA Technologies) containing the sgRNA  
578 expression cassette (with the optimized sgRNA scaffold<sup>35</sup>) were inserted in pCCL.AS3m generating  
579 the transfer vectors (pCCL.AS3m.gRs) for the LV production.

580 Third-generation lentiviral vectors were produced by calcium phosphate transient  
581 transfection of HEK293T cells with the transfer vector (pCCL.AS3m or pCCL.AS3m.gRs), the

582 packaging plasmid pKLg/p.RRE, the Rev-encoding plasmid pK.REV, and the vesicular stomatitis  
583 virus glycoprotein G (VSV-G) envelope-encoding plasmid pK.G. The physical titer of vector  
584 preparations was measured using the HIV-1 Gag p24 antigen immunocapture assay kit  
585 (PerkinElmer, Waltham, MA, USA) and expressed as p24 ng/mL. The viral infectious titer was  
586 calculated by transducing HCT116 cells with serial vector dilutions, as previously described<sup>77</sup>.  
587 Vector copy number per diploid genome (VCN) was calculated to determine the viral infectious  
588 titer, expressed as transducing units *per* ml (TU/mL). Viral infectivity was calculated as ratio  
589 between infectious and physical titers (TU/ng p24).

590

### 591 **HSPC transduction and transfection**

592 We isolated cord blood CD34<sup>+</sup> HSPCs and adult G-CSF-mobilized HSPCs from healthy donors.  
593 Human adult CD34<sup>+</sup> HSPCs were isolated from the blood of SCD patients either after Plerixafor-  
594 mobilization (NCT 02212535 clinical trial, Necker Hospital, Paris, France) or after  
595 erythrocytapheresis. Written informed consent was obtained from all the subjects. All experiments  
596 were performed in accordance with the Declaration of Helsinki. The study was approved by the  
597 regional investigational review board (reference: DC 2014-2272, CPP Ile-de-France II “Hôpital  
598 Necker-Enfants malades”). HSPCs were purified by immuno-magnetic selection with AutoMACS  
599 (Miltenyi Biotec) after immunostaining with CD34 MicroBead Kit (Miltenyi Biotec). CD34<sup>+</sup> cells  
600 were cultured (10<sup>6</sup> cells/ml) 24 h before transduction in X-VIVO 20 supplemented with  
601 penicillin/streptomycin (Gibco, Carlsbad, CA, USA), StemRegenin1 at 250 nM (SR1; StemCell  
602 Technologies) and the following recombinant human cytokines (Peprotech): 300 ng/mL SCF, 300  
603 ng/mL Flt-3L, 100 ng/mL TPO and 60 ng/mL IL3 (“expansion medium”).

604 Two hours before LV transduction, CD34<sup>+</sup> cells were plated in RetroNectin-coated plates  
605 (10 µg/cm<sup>2</sup>, Takara Bio, Kusatsu, Japan) at 3x10<sup>6</sup> cells/ml in the expansion medium supplemented  
606 with 16,16-dimethyl-prostaglandin E2 (10 µM PGE2; Cayman Chemical)<sup>78</sup>. Cells were then  
607 transduced for 24 h in the expansion medium supplemented with protamine sulfate (4 µg/ml,

608 Sigma-Aldrich, St. Louis, MI, USA or APP Pharmaceuticals, Schaumburg, IL, USA), PGE2 and  
609 LentiBOOST( Sirion Biotech<sup>70</sup>). After expansion of CD34<sup>+</sup> cells for 48h, 100.000 cells were  
610 transfected with 15 µg Cas9-GFP protein (provided by Dr. De Cian) by using the P3 Primary Cell  
611 4D-Nucleofector X Kit S (Lonza) and the AMAXA 4D CA137 program (Lonza). After  
612 transfection, cells were plated at a concentration of 50,000 cells/mL in the erythroid differentiation  
613 medium.

614

### 615 **Erythroid differentiation of HSPCs**

616 After transfection, HSPCs were differentiated into mature RBCs using a 3-phase protocol<sup>44</sup>. From  
617 day 0 to day 6, cells were grown in a basal erythroid medium<sup>6</sup> supplemented with 10<sup>-6</sup> M  
618 hydrocortisone (Sigma), 100 ng/mL SCF (Peprotech), 5 ng/mL IL3 (Peprotech), and 3 IU/mL of  
619 EPO (Eprex, Janssen-Cilag). From day 6 to day 9, cells were cultured onto a layer of murine  
620 stromal MS-5 cells in the basal erythroid medium supplemented only with 3 IU/mL EPO. Finally,  
621 from day 9 to day 20, cells were cultured on a layer of MS-5 cells in the basal erythroid medium  
622 without any cytokines. Erythroid differentiation and enucleation rate were monitored by flow  
623 cytometry analysis.

624

### 625 **Reverse phase and cation-exchange HPLC analysis**

626 For HPLC analyses, HUDEP-2 cells were collected at day 9 of erythroid differentiation, whereas *in*  
627 *vitro* differentiated RBCs were collected at day 20 of erythroid differentiation.

628 Reverse phase (RP) HPLC analysis were performed using a NexeraX2 SIL-30AC  
629 chromatograph (Shimadzu) and the LC Solution software. Globin chains were separated by HPLC  
630 using a 250x4.6 mm, 3.6 µm Aeris Widepore column (Phenomenex). Samples were eluted with a  
631 gradient mixture of solution A (water/acetonitrile/trifluoroaceticacid, 95:5:0.1) and solution  
632 B (water/acetonitrile/trifluoroacetic acid, 5:95:0.1). The absorbance was measured at 220 nm.

633 Cation-exchange (CE) HPLC analysis were performed using a NexeraX2 SIL-30AC  
634 chromatograph (Shimadzu) and the LC Solution software. Hemoglobin tetramers were separated by  
635 HPLC using a 2 cation-exchange column (PolyCAT A, PolyLC, Coulmbia, MD). Samples were  
636 eluted with a gradient mixture of solution A (20mM bis Tris, 2mM KCN, pH=6.5) and solution  
637 B (20mM bis Tris, 2mM KCN, 250mM NaCl, pH=6.8). The absorbance was measured at 415 nm.

638

### 639 **Sickling assay**

640 *In vitro* differentiated RBCs (day 19-20 of differentiation) derived from treated and control SCD  
641 HSPCs were exposed to an oxygen-deprived atmosphere (0% O<sub>2</sub>) and the time-course of sickling  
642 was monitored in real-time by video microscopy for 1 hour, capturing images every 20 minutes  
643 using the AxioObserver Z1 microscope (Zeiss) and a 40X objective. At 0% O<sub>2</sub>, around 400 cells per  
644 condition were counted and processed with ImageJ to determine the percentage of sickled RBCs in  
645 the total cell population.

646

### 647 **Quantitative phase image microscopy of RBCs**

648 50,000 to 100,00 *in vitro* differentiated RBCs were centrifuged at 1,500 rpm for 5 min, resuspended  
649 in 50 µL of PBS 0.5% BSA, and placed in a µ-Slide with 15 or 8 wells (Ibidi). We used the SID4  
650 HR GE camera (Phasics, Saint-Aubin, France) with an inverted microscope (Eclipse Ti-E, Nikon)  
651 to obtain quantitative phase images of label-free RBCs<sup>80</sup>. Pictures were taken using a 40X/0.60  
652 objective. The BIO-Data R&D software (version 2.7.1.46) performed a segmentation procedure to  
653 isolate each RBC from a picture. We analyzed only enucleated RBCs, discarding cells with a  
654 surface density (dry mass/surface) higher than 0.55 pg/µm<sup>2</sup>. For each RBC, we evaluated dry mass  
655 (pg), surface (µm<sup>2</sup>), perimeter (µm) and ellipticity<sup>81</sup>.

656

### 657 **Statistics**

658 Data were analyzed with Graph Pad Prism software (version 7.0) and expressed as mean  $\pm$  standard  
659 error mean (SEM), if not otherwise stated. Parametric tests (Student's t-test, unpaired t tests, Two-  
660 or One-way ANOVA test, Sidak's, Dunnett's and Tukey's multiple comparisons test) were used  
661 according to datasets. The threshold for statistical significance was set to  $P < 0.05$ . Linear or non-  
662 linear regression analyses were performed to assess the correlation between frequency of genome  
663 editing and VCN or between frequency of genome editing or VCN and Hb expression.

664

665 **Author contributions**

666

667 Contribution: S.R. designed and performed experiments, analyzed data, and wrote the paper; A.C.,  
668 T.F., S.E., A.Ca. and G.M. performed experiments and analyzed data; N.O. and S.A. analyzed  
669 quantitative phase microscopy, C.M. analyzed off-target NGS data; S.F. and A.D.C. provided  
670 reagents; J.P.C., M.C., A.Ce., W.E.N., M.A. and B.W. contributed to the design of the experimental  
671 strategy; V.M. conceived the study, designed and performed experiments, analyzed data, and wrote  
672 the paper; A.M. conceived the study, designed experiments, analyzed data, and wrote the paper.

673

674 **Acknowledgments**

675

676 This work was supported by State funding from the Agence Nationale de la Recherche under  
677 “Investissements d’avenir” program (ANR-10-IAHU-01), the Paris Ile de France Region under  
678 “DIM Thérapie génique” initiative, the Société d’Accélération du Transfert de Technologies-SATT  
679 IDF Innov, the Fondation maladies rare and the Sanofi Innovation Award. We thank Sylvie Fabrega  
680 (Plateforme Vecteurs Viraux et Transfert de Gènes, SFR Necker, US 24, UMS 3633, 75014 Paris,  
681 France) for the LV production.

682

683 **Conflicts of interests**

684

685 V.M. and A.M. are the inventors of 2 patents describing this gene addition/genome editing platform  
686 (WO/2018/220211: “Viral vectors combining gene therapy and genome editing approaches for gene  
687 therapy of genetic disorders”; WO/2018/220210: “Recombinant lentiviral vector for stem cell-based  
688 gene therapy of sickle cell disorder). All other authors declare no competing interests.

689

690 **Keywords**

691

692 Lentiviral vectors, genome editing, CRISPR/Cas9 nuclease, sickle cell disease.

693

694 **References**

695

696 1. Cavazzana M, Antoniani C, Miccio A. Gene Therapy for  $\beta$ -Hemoglobinopathies. *Molecular*  
697 *Therapy*. 2017;25(5):1142–1154.

698 2. Ngo S, Bartolucci P, Lobo D, et al. Causes of Death in Sickle Cell Disease Adult Patients:  
699 Old and New Trends. *Blood*. 2014;124(21):2715–2715.

700 3. Sadelain M, Boulad F, Galanello R, et al. Therapeutic options for patients with severe beta-  
701 thalassemia: the need for globin gene therapy. *Hum Gene Ther*. 2007;18(1):1–9.

702 4. Besse K, Maiers M, Confer D, Albrecht M. On Modeling Human Leukocyte Antigen-  
703 Identical Sibling Match Probability for Allogeneic Hematopoietic Cell Transplantation: Estimating  
704 the Need for an Unrelated Donor Source. *Biol Blood Marrow Transplant*. 2016;22(3):410–417.

705 5. Miccio A, Cesari R, Lotti F, et al. In vivo selection of genetically modified erythroblastic  
706 progenitors leads to long-term correction of  $\beta$ -thalassemia. *Proc Natl Acad Sci U S A*.  
707 2008;105(30):10547–10552.

708 6. Weber L, Poletti V, Magrin E, et al. An Optimized Lentiviral Vector Efficiently Corrects the  
709 Human Sickle Cell Disease Phenotype. *Molecular Therapy - Methods & Clinical Development*.  
710 2018;10:268–280.

711 7. Ribeil J-A, Hacein-Bey-Abina S, Payen E, et al. Gene Therapy in a Patient with Sickle Cell  
712 Disease. *New England Journal of Medicine*. 2017;376(9):848–855.

713 8. Magrin E, Miccio A, Cavazzana M. Lentiviral and genome-editing strategies for the  
714 treatment of  $\beta$ -hemoglobinopathies. *Blood reviews*. 2019;11.

- 715 9. Cavazzana-Calvo M, Payen E, Negre O, et al. Transfusion independence and HMGA2  
716 activation after gene therapy of human  $\beta$ -thalassaemia. *Nature*. 2010;467(7313):318–322.
- 717 10. Kaiser J, 2021, Pm 6:15. Gene therapy trials for sickle cell disease halted after two patients  
718 develop cancer. *Science | AAAS*. 2021;
- 719 11. Markt S, Scaramuzza S, Cicalese MP, et al. Intrabone hematopoietic stem cell gene  
720 therapy for adult and pediatric patients affected by transfusion-dependent  $\beta$ -thalassemia. *Nat Med*.  
721 2019;25(2):234–241.
- 722 12. Miccio A, Poletti V, Tiboni F, et al. The GATA1-HS2 enhancer allows persistent and  
723 position-independent expression of a  $\beta$ -globin transgene. *PLoS One*. 2011;6(12):e27955.
- 724 13. Levasseur DN, Ryan TM, Reilly MP, et al. A Recombinant Human Hemoglobin with Anti-  
725 sickling Properties Greater than Fetal Hemoglobin. *J. Biol. Chem*. 2004;279(26):27518–27524.
- 726 14. Dever DP, Bak RO, Reinisch A, et al. CRISPR/Cas9  $\beta$ -globin gene targeting in human  
727 haematopoietic stem cells. *Nature*. 2016;539(7629):384–389.
- 728 15. Wilkinson AC, Dever DP, Baik R, et al. Cas9-AAV6 gene correction of beta-globin in  
729 autologous HSCs improves sickle cell disease erythropoiesis in mice. *Nat Commun*.  
730 2021;12(1):686.
- 731 16. Park SH, Lee CM, Dever DP, et al. Highly efficient editing of the  $\beta$ -globin gene in patient-  
732 derived hematopoietic stem and progenitor cells to treat sickle cell disease. *Nucleic Acids Research*.  
733 2019;47(15):7955–7972.
- 734 17. Genovese P, Schirotti G, Escobar G, et al. Targeted genome editing in human repopulating  
735 haematopoietic stem cells. *Nature*. 2014;510(7504):235–240.
- 736 18. Magis W, DeWitt MA, Wyman SK, et al. High-level correction of the sickle mutation  
737 amplified in vivo during erythroid differentiation. *bioRxiv*. 2019;432716.
- 738 19. Forget BG. Molecular Basis of Hereditary Persistence of Fetal Hemoglobin. *Annals NY*  
739 *Acad Sci*. 1998;850(1 COOLEY'S ANEM):38–44.
- 740 20. Traxler EA, Yao Y, Wang Y-D, et al. A genome-editing strategy to treat  $\beta$ -

- 741 hemoglobinopathies that recapitulates a mutation associated with a benign genetic condition. *Nature*  
742 *Medicine*. 2016;22(9):987–990.
- 743 21. Li C, Psatha N, Sova P, et al. Reactivation of  $\gamma$ -globin in adult  $\beta$ -YAC mice after ex vivo  
744 and in vivo hematopoietic stem cell genome editing. *Blood*. 2018;131(26):2915–2928.
- 745 22. Lux CT, Pattabhi S, Berger M, et al. TALEN-Mediated Gene Editing of HBG in Human  
746 Hematopoietic Stem Cells Leads to Therapeutic Fetal Hemoglobin Induction. *Mol Ther Methods*  
747 *Clin Dev*. 2019;12:175–183.
- 748 23. Weber L, Frati G, Felix T, et al. Editing a  $\gamma$ -globin repressor binding site restores fetal  
749 hemoglobin synthesis and corrects the sickle cell disease phenotype. *Sci. Adv*. 2020;6(7):eaay9392.
- 750 24. Antoniani C, Meneghini V, Lattanzi A, et al. Induction of fetal hemoglobin synthesis by  
751 CRISPR/Cas9-mediated editing of the human  $\beta$ -globin locus. *Blood*. 2018;131(17):1960–1973.
- 752 25. Brendel C, Guda S, Renella R, et al. Lineage-specific BCL11A knockdown circumvents  
753 toxicities and reverses sickle phenotype. *J Clin Invest*. 2016;126(10):3868–3878.
- 754 26. Canver MC, Smith EC, Sher F, et al. BCL11A enhancer dissection by Cas9-mediated in situ  
755 saturating mutagenesis. *Nature*. 2015;527(7577):192–197.
- 756 27. Chang K-H, Smith SE, Sullivan T, et al. Long-Term Engraftment and Fetal Globin  
757 Induction upon BCL11A Gene Editing in Bone-Marrow-Derived CD34 + Hematopoietic Stem and  
758 Progenitor Cells. *Molecular Therapy - Methods & Clinical Development*. 2017;4:137–148.
- 759 28. Frangoul H, Altshuler D, Cappellini MD, et al. CRISPR-Cas9 Gene Editing for Sickle Cell  
760 Disease and  $\beta$ -Thalassemia. *New England Journal of Medicine*. 2021;384(3):252–260.
- 761 29. Liang P, Xu Y, Zhang X, et al. CRISPR/Cas9-mediated gene editing in human triploid zygotes.  
762 *Protein Cell*. 2015;6(5):363–372.
- 763 30. Cradick TJ, Fine EJ, Antico CJ, Bao G. CRISPR/Cas9 systems targeting  $\beta$ -globin and CCR5  
764 genes have substantial off-target activity. *Nucleic Acids Research*. 2013;41(20):9584–9592.
- 765 31. Kurita R, Suda N, Sudo K, et al. Establishment of Immortalized Human Erythroid  
766 Progenitor Cell Lines Able to Produce Enucleated Red Blood Cells. *PLoS One*. 2013;8(3):.

- 767 32. Brinkman EK, Chen T, Amendola M, van Steensel B. Easy quantitative assessment of  
768 genome editing by sequence trace decomposition. *Nucleic Acids Res.* 2014;42(22):e168.
- 769 33. Luo Y, Zhu D, Zhang Z, Chen Y, Sun X. Integrative Analysis of CRISPR/Cas9 Target Sites  
770 in the Human HBB Gene. *Biomed Res Int.* 2015;2015:.
- 771 34. Cradick TJ, Qiu P, Lee CM, Fine EJ, Bao G. COSMID: A Web-based Tool for Identifying  
772 and Validating CRISPR/Cas Off-target Sites. *Mol Ther Nucleic Acids.* 2014;3(12):e214.
- 773 35. Dang Y, Jia G, Choi J, et al. Optimizing sgRNA structure to improve CRISPR-Cas9  
774 knockout efficiency. *Genome Biology.* 2015;15;16:280.
- 775 36. Pavani G, Fabiano A, Laurent M, et al. Correction of  $\beta$ -thalassemia by CRISPR/Cas9 editing  
776 of the  $\alpha$ -globin locus in human hematopoietic stem cells. *Blood Advances.* 2021;5(5):1137–1153.
- 777 37. Roselli EA, Mezzadra R, Frittoli MC, et al. Correction of beta-thalassemia major by gene  
778 transfer in haematopoietic progenitors of pediatric patients. *EMBO Mol Med.* 2010;2(8):315–328.
- 779 38. Esrick EB, Lehmann LE, Biffi A, et al. Post-Transcriptional Genetic Silencing of BCL11A  
780 to Treat Sickle Cell Disease. *New England Journal of Medicine.* 2021;384(3):205–215.
- 781 39. Ahle S. Gene Editing Therapy Shows Early Benefit for Patients With SCD and Beta  
782 Thalassemia. *ASH Clinical News-Latest Online Exclusives.* 2020;
- 783 40. Smith AR, Schiller GJ, Vercellotti GM, et al. Preliminary Results of a Phase 1/2 Clinical  
784 Study of Zinc Finger Nuclease-Mediated Editing of BCL11A in Autologous Hematopoietic Stem  
785 Cells for Transfusion-Dependent Beta Thalassemia. *Blood.* 2019;134(Supplement\_1):3544–3544.
- 786 41. Sankaran VG, Menne TF, Xu J, et al. Human Fetal Hemoglobin Expression Is Regulated by  
787 the Developmental Stage-Specific Repressor *BCL11A*. *Science.* 2008;322(5909):1839–1842.
- 788 42. Yin J, Xie X, Ye Y, Wang L, Che F. BCL11A: a potential diagnostic biomarker and  
789 therapeutic target in human diseases. *Biosci Rep.* 2019;39(11):.
- 790 43. Lattanzi A, Meneghini V, Pavani G, et al. Optimization of CRISPR/Cas9 Delivery to  
791 Human Hematopoietic Stem and Progenitor Cells for Therapeutic Genomic Rearrangements.  
792 *Molecular Therapy.* 2018;

- 793 44. Giarratana M-C, Kobari L, Lapillonne H, et al. Ex vivo generation of fully mature human  
794 red blood cells from hematopoietic stem cells. *Nature Biotechnology*. 2005;23(1):69–74.
- 795 45. Galanello R, Origa R. Beta-thalassemia. *Orphanet J Rare Dis*. 2010;5:11.
- 796 46. Needs T, Gonzalez-Mosquera LF, Lynch DT. Beta Thalassemia. *StatPearls*. 2021;
- 797 47. Thompson AA, Walters MC, Kwiatkowski J, et al. Gene Therapy in Patients with  
798 Transfusion-Dependent  $\beta$ -Thalassemia. *New England Journal of Medicine*. 2018;
- 799 48. Tisdale JF, Thompson AA, Kwiatkowski JL, et al. Abstract 196. Updated Results from  
800 HGB-206 LentiGlobin for Sickle Cell Disease Gene Therapy Study: Group C Data and Group A  
801 AML Case Investigation. *Molecular Therapy*. 2021;29(4):1–427.
- 802 49. Seminog OO, Ogunlaja OI, Yeates D, Goldacre MJ. Risk of individual malignant neoplasms  
803 in patients with sickle cell disease: English national record linkage study. *J R Soc Med*.  
804 2016;109(8):303–309.
- 805 50. Brunson A, Keegan THM, Bang H, et al. Increased risk of leukemia among sickle cell  
806 disease patients in California. *Blood*. 2017;130(13):1597–1599.
- 807 51. Breda L, Ghiaccio V, Tanaka N, et al. Lentiviral vector ALS20 yields high hemoglobin  
808 levels with low genomic integrations for treatment of beta-globinopathies. *Mol Ther*.  
809 2021;29(4):1625–1638.
- 810 52. Akinsheye I, Alsultan A, Solovieff N, et al. Fetal hemoglobin in sickle cell anemia. *Blood*.  
811 2011;118(1):19–27.
- 812 53. Steinberg MH, Chui DHK, Dover GJ, Sebastiani P, Alsultan A. Fetal hemoglobin in sickle  
813 cell anemia: a glass half full? *Blood*. 2014;123(4):481–485.
- 814 54. Yudovich D, Bäckström A, Schmiderer L, et al. Combined lentiviral- and RNA-mediated  
815 CRISPR/Cas9 delivery for efficient and traceable gene editing in human hematopoietic stem and  
816 progenitor cells. *Sci Rep*. 2020;10(1):22393.
- 817 55. Ting PY, Parker AE, Lee JS, et al. Guide Swap enables genome-scale pooled CRISPR–Cas9  
818 screening in human primary cells. *Nature Methods*. 2018;

- 819 56. Martyn GE, Wienert B, Yang L, et al. Natural regulatory mutations elevate the fetal globin  
820 gene via disruption of BCL11A or ZBTB7A binding. *Nat Genet.* 2018;50(4):498–503.
- 821 57. Liu N, Xu S, Yao Q, et al. Transcription factor competition at the  $\gamma$ -globin promoters  
822 controls hemoglobin switching. *Nat Genet.* 2021;53(4):511–520.
- 823 58. Chaudhari HG, Penterman J, Whitton HJ, et al. Evaluation of Homology-Independent  
824 CRISPR-Cas9 Off-Target Assessment Methods. *CRISPR J.* 2020;3(6):440–453.
- 825 59. Shapiro J, Iancu O, Jacobi AM, et al. Increasing CRISPR Efficiency and Measuring Its  
826 Specificity in HSPCs Using a Clinically Relevant System. *Mol Ther Methods Clin Dev.*  
827 2020;17:1097–1107.
- 828 60. Tsai SQ, Joung JK. Defining and improving the genome-wide specificities of CRISPR-Cas9  
829 nucleases. *Nat Rev Genet.* 2016;17(5):300–312.
- 830 61. Wu Y, Zeng J, Roscoe BP, et al. Highly efficient therapeutic gene editing of human  
831 hematopoietic stem cells. *Nature Medicine.* 2019;25(5):776–783.
- 832 62. Gaziev J, Lucarelli G. Stem cell transplantation for hemoglobinopathies. *Curr Opin Pediatr.*  
833 2003;15(1):24–31.
- 834 63. Cromer MK, Vaidyanathan S, Ryan DE, et al. Global Transcriptional Response to  
835 CRISPR/Cas9-AAV6-Based Genome Editing in CD34+ Hematopoietic Stem and Progenitor Cells.  
836 *Mol Ther.* 2018;26(10):2431–2442.
- 837 64. Uchida N, Drysdale CM, Nassehi T, et al. Cas9 protein delivery non-integrating lentiviral  
838 vectors for gene correction in sickle cell disease. *Molecular Therapy - Methods & Clinical*  
839 *Development.* 2021;21:121–132.
- 840 65. Chang HHY, Pannunzio NR, Adachi N, Lieber MR. Non-homologous DNA end joining and  
841 alternative pathways to double-strand break repair. *Nat Rev Mol Cell Biol.* 2017;18(8):495–506.
- 842 66. Hustedt N, Durocher D. The control of DNA repair by the cell cycle. *Nat Cell Biol.*  
843 2017;19(1):1–9.
- 844 67. Nakamura K, Saredi G, Becker JR, et al. H4K20me0 recognition by BRCA1–BARD1

845 directs homologous recombination to sister chromatids. *Nat Cell Biol.* 2019;21(3):311–318.

846 68. Vitor AC, Huertas P, Legube G, de Almeida SF. Studying DNA Double-Strand Break  
847 Repair: An Ever-Growing Toolbox. *Front. Mol. Biosci.* 2020;7:24.

848 69. Magis W, DeWitt MA, Wyman SK, et al. High-level correction of the sickle mutation  
849 amplified in vivo during erythroid differentiation. *bioRxiv.* 2018;

850 70. Frangoul H. Safety and Efficacy of CTX001 in Patients with Transfusion-Dependent  $\beta$ -  
851 Thalassemia and Sickle Cell Disease: Early Results from the Climb THAL-111 and Climb SCD-  
852 121 Studies of Autologous CRISPR-CAS9–Modified CD34+ Hematopoietic Stem and Progenitor  
853 Cells. 2020;

854 71. Gaudelli NM, Lam DK, Rees HA, et al. Directed evolution of adenine base editors with  
855 increased activity and therapeutic application. *Nat Biotechnol.* 2020;38(7):892–900.

856 72. Richter MF, Zhao KT, Eton E, et al. Phage-assisted evolution of an adenine base editor with  
857 improved Cas domain compatibility and activity. *Nat Biotechnol.* 2020;38(7):883–891.

858 73. Rees HA, Liu DR. Base editing: precision chemistry on the genome and transcriptome of  
859 living cells. *Nat Rev Genet.* 2018;19(12):770–788.

860 74. Nakamura M, Gao Y, Dominguez AA, Qi LS. CRISPR technologies for precise epigenome  
861 editing. *Nat Cell Biol.* 2021;23(1):11–22.

862 75. Anzalone AV, Randolph PB, Davis JR, et al. Search-and-replace genome editing without  
863 double-strand breaks or donor DNA. *Nature.* 2019;576(7785):149–157.

864 76. Hardison R, Slightom JL, Gumucio DL, et al. Locus control regions of mammalian beta-  
865 globin gene clusters: combining phylogenetic analyses and experimental results to gain functional  
866 insights. *Gene.* 1997;205(1–2):73–94.

867 77. Lattanzi A, Duguez S, Moiani A, et al. Correction of the Exon 2 Duplication in DMD  
868 Myoblasts by a Single CRISPR/Cas9 System. *Mol Ther Nucleic Acids.* 2017;7:11–19.

869 78. Zonari E, Desantis G, Petrillo C, et al. Efficient Ex Vivo Engineering and Expansion of  
870 Highly Purified Human Hematopoietic Stem and Progenitor Cell Populations for Gene Therapy.

871 *Stem Cell Reports*. 2017;8(4):977–990.

872 79. Delville M, Soheili T, Bellier F, et al. A Nontoxic Transduction Enhancer Enables Highly  
873 Efficient Lentiviral Transduction of Primary Murine T Cells and Hematopoietic Stem Cells. *Mol*  
874 *Ther Methods Clin Dev*. 2018;10:341–347.

875 80. Bon P, Maucort G, Wattellier B, Monneret S. Quadriwave lateral shearing interferometry for  
876 quantitative phase microscopy of living cells. *Opt. Express*. 2009;17(15):13080.

877 81. Aknoun S, Savatier J, Bon P, et al. Living cell dry mass measurement using quantitative  
878 phase imaging with quadriwave lateral shearing interferometry: an accuracy and sensitivity  
879 discussion. *J. Biomed. Opt.* 2015;20(12):126009.

880

881

## 882 **Figure Legends**

883

### 884 **Figure 1: Test and validation of an effective sgRNA to knock-down the *HBB* gene.**

885 (A) sgRNAs are aligned to their complementary on-target loci on exon 1 of the *HBB* gene. gR-B  
886 targets a region containing the SCD mutation, therefore its sequence was modified to target the WT  
887 *HBB* gene during the validation experiments in K562 and HUDEP-2 erythroid cell lines, and in HD  
888 HSPCs. The codon containing the SCD mutation is highlighted in red. (B) Editing efficiency by  
889 TIDE analysis after PCR amplification of the target region and Sanger sequencing in Cas9-GFP<sup>+</sup>  
890 K562 (n=3 for gR-A, 4 for gR-B, 6 for gR-C and 5 for gR-D) and HUDEP-2 (n=5 for gR-C; n=4  
891 for gR-A, B and D) erythroid cell lines. Transfection efficiency was 55-70% for K562 and 30-60%  
892 for HUDEP-2. Data are expressed as mean±SEM (C) Out-of-frame mutations identified using  
893 TIDE after PCR amplification of the target region and Sanger sequencing in K562 (n=3 for gR-A, 4  
894 for gR-B, 6 for gR-C and 5 for gR-D) and HUDEP-2 (n=5 for gR-C; n=4 for gR-A, B and D)  
895 erythroid cell lines. Data are expressed as mean±SEM. The frequency of out-of-frame mutations for  
896 gR-C was significantly higher than for gR-A (p < 0.0001 in K562 and p < 0.05 in HUDEP-2) and  
897 gR-B (p < 0.005 in K562). In K562, the frequency of out-of-frame mutations for gR-D was  
898 significantly higher than for gR-A and gR-B (p < 0.0005). In both K562 and HUDEP-2, no  
899 differences were observed between gR-C and gR-D (One-way ANOVA test – Tukey’s multiple  
900 comparisons test). (D) Relative expression of *HBB*, *HBD* and *HBG* mRNAs normalized to  $\alpha$ -globin,  
901 detected by RT-qPCR in HUDEP-2 cells. Data are expressed as mean±SEM (n=3). \*\* p < 0.01  
902 between gR-A or gR-B vs Ctr-Cas9. \*\*\* p < 0.001 between gR-C or gR-D vs Ctr-Cas9 (Two-way  
903 ANOVA test – Dunnett’s multiple comparisons test). Ctr-Cas9 samples are HUDEP-2 cells  
904 transfected only with the Cas9-GFP plasmid. (E) Relative expression of the  $\beta$ -globin chain  
905 normalized to the  $\alpha$ -globin chain, as measured by Western blot analysis in differentiated HUDEP-2  
906 cells. Data are expressed as mean±SEM (n=4 for gR-C; n=3 for gR-A, B and D) \* p < 0.05 and \*\* p  
907 < 0.01 vs Ctr-Cas9 (Two-way ANOVA test - Sidak’s multiple comparisons test). A representative

908 western blot image is shown. Ctr-Cas9 samples are HUDEP-2 cells transfected only with the Cas9-  
909 GFP plasmid. (F) Editing efficiency (InDels) and frequency of out-of-frame mutations measured by  
910 TIDE analysis after PCR amplification of the target region and Sanger sequencing in G-CSF-  
911 mobilized peripheral blood (mPB) HD HSPCs edited with gR-C (n=1 for HD1, n=2 for HD2 and  
912 n=2 for HD3). Data are expressed as mean±SEM. (G) Relative expression of *HBB*, *HBD* and *HBG*  
913 mRNAs normalized to  $\alpha$ -globin, measured by RT-qPCR in erythroid cells derived from G-CSF-  
914 mPB HD HSPCs transfected with Cas9-GFP plasmid only (Ctr-Cas9) or with both Cas9-GFP and  
915 gR-C plasmids (gR-C). *HBB* decrease upon gR-C treatment is reported as percentage above the  
916 histogram bars. (n=1 for HD1, n=2 for HD2 and n=2 for HD3). Data are expressed as mean±SEM.  
917 (H) RP-HPLC quantification of globin chains in erythroid cells derived from G-CSF-mPB HD  
918 HSPCs transfected with Cas9-GFP plasmid only (Ctr-Cas9) or with both Cas9-GFP and gR-C  
919 plasmids (gR-C).  $\beta$ -like globin chains are normalized over  $\alpha$ -globin chains (n=1 for HD1, n=2 for  
920 HD2 and n=2 for HD3; n= 5 biological replicates). The percentage of  $\beta$ -globin decrease upon gR-C  
921 treatment and the  $\alpha$ -non- $\alpha$ -globin ratio are reported above the histogram bars. Data are expressed as  
922 mean±SEM. A representative chromatogram is reported in the left panel. (I) CE-HPLC analysis of  
923 Hb tetramers in  $\beta$ -thalassemic cells (thal) and in erythroid cells derived from G-CSF-mPB HD  
924 HSPCs treated or not with gR-C. gR-C treated samples have a hemoglobin expression pattern  
925 similar to the profile observed in *in vitro* differentiated erythroid cells from a  $\beta$ -thalassemia patient.  
926 We calculated the percentage of Hb types over the total Hb tetramers (n=2 donors). CE-HPLC  
927 chromatograms are reported on the left panel.  $\alpha$ P= $\alpha$ -precipitates.

928

929 **Figure 2: Combination of lentiviral and genome editing technologies is efficient in HUDEP-2**  
930 **cells.**

931 (A) Schematic representation of the LVs carrying either the AS3 globin gene (LV AS3, strategy #1)  
932 or the AS3m globin gene and a sgRNA-expressing cassette (LV AS3m.gR). Both AS3- and AS3m-  
933 globin genes are under the control of a short  $\beta$ -globin promoter ( $\beta$ -p) and a mini- $\beta$ LCR containing

934 HS2 and HS3. The anti-sickling amino acid substitutions are reported in red. The modified  
935 nucleotides in LV AS3m, avoiding its targeting by the gR-C, are reported in green. We indicated  
936 the amino acids below the nucleotide sequence. sgRNA expression is under the control of the  
937 human U6 promoter (U6p). gR-C targets a region in exon 1 (Ex1) of *HBB* (strategy # 2), gR-  
938 *BCL11A* targets the +58kb erythroid-specific enhancer of *BCL11A* (strategy # 3) and gR-13bpdel  
939 targets the *BCL11A* binding site within the *HBG* promoters (strategy # 4). **(B)** Schematic  
940 representation of the LV transduction and plasmid transfection protocol used in HUDEP-2 cells.  
941 Cells were transduced with LV AS3m carrying gR-C, *BCL11A* and 13bpdel sgRNAs and  
942 transfected after 10 days with a Cas9-GFP plasmid. Transfection efficiency was 30-60%. FACS-  
943 sorted Cas9-GFP<sup>+</sup> cells were differentiated into mature erythroblasts. **(C)** Relative expression of  
944 *HBB* and *AS3m* mRNAs normalized to  $\alpha$ -globin, as detected by qRT-PCR. Data are expressed as  
945 mean $\pm$ SEM. VCN are reported in blue and InDels in black below the graph. Ctr UT are untreated  
946 HUDEP-2 cells and Ctr TE are HUDEP-2 cells transfected only with TE buffer. Transduced  
947 samples that were mock-transfected, are indicated with “-”. The percentage of *HBB* decrease upon  
948 LV AS3m.C treatment is reported above the histogram bars. Data are expressed as mean $\pm$ SEM. **(D)**  
949 RP-HPLC quantification of globin chains in Cas9-treated and control (mock transfected) LV  
950 AS3m.C-transduced cells.  $\beta$ -like globin chains were normalized to  $\alpha$ -globin chains. VCN are  
951 reported in blue and InDels in black below the graph. Ctr UT are untreated HUDEP-2 cells and Ctr  
952 TE are HUDEP-2 cells transfected only with TE buffer. Transduced samples that were mock-  
953 transfected, are indicated with “-” and harbored no InDels. The percentage of  $\beta$ -globin decrease  
954 upon LV AS3m.C treatment and the  $\alpha$ -/ $\text{non-}\alpha$ -globin ratio are reported above the histogram bars.  
955 **(E)** CE-HPLC chromatograms (left panel) and quantification (right panel) of Hb tetramers in Cas9-  
956 treated and control mock-transfected LV AS3m.C-transduced cells. We calculated the percentage of  
957 each Hb type over the total Hb tetramers. VCN are reported in blue and InDels in black below the  
958 graph. Ctr UT are untreated HUDEP-2 cells and Ctr TE are HUDEP-2 cells transfected only with  
959 TE buffer. The decrease in HbA expression upon LV AS3m.C treatment is reported as percentage

960 above the histogram bars. **(F)** Editing efficiency (InDel frequency) in LV AS3m.C-treated HUDEP-  
961 2 cells measured by TIDE analysis after PCR amplification and Sanger sequencing of the target  
962 region in *HBB* exon 1 and the potential off-target region in the transgene (AS3m) in Cas9-GFP<sup>+</sup>  
963 HUDEP-2 erythroid cells. **(G)** Relative *HBG* expression normalized to  $\alpha$ -globin, as detected by RT-  
964 qPCR in Cas9-treated and mock-transfected cells transduced with LV AS3m.BCL11A or LV  
965 AS3m.13bpdel. VCN are reported in blue and InDels in black below the graph. Ctr UT are  
966 untreated HUDEP-2 cells and Ctr TE are HUDEP-2 cells transfected only with TE buffer. Data are  
967 expressed as mean $\pm$ SEM. **(H)** RP-HPLC quantification of globin chains in Cas9-treated and mock-  
968 transfected cells transduced with LV AS3m.BCL11A or LV AS3m.13bpdel.  $\beta$ -like globin chains  
969 are normalized over  $\alpha$ -globin. VCN are reported in blue and InDels in black below the graph.  $\alpha$ -  
970 /non- $\alpha$ -globin ratios are reported above the histogram bars. Ctr UT are untreated HUDEP-2 cells  
971 and Ctr TE are HUDEP-2 cells transfected only with TE buffer. **(I)** CE-HPLC chromatograms (left  
972 panel) and quantification (right panel) of Hb tetramers in Cas9-treated and mock-transfected LV  
973 AS3m.BCL11A- and LV AS3m.13bpdel-transduced cells. We plotted the percentage of each Hb  
974 type over the total Hb tetramers. VCN are reported in blue and InDels in black below the graph. The  
975 percentage of HbA decrease is reported above the histogram bars. Ctr UT are untreated HUDEP-2  
976 cells and Ctr TE are HUDEP-2 cells transfected only with TE buffer.

977

978 **Figure 3: Testing of the bifunctional LV AS3m.C in SCD HSPCs.**

979 **(A)** Schematic representation of the protocol used to transduce and transfect SCD HSPCs. 24h after  
980 thawing, HSPCs were transduced with LV AS3m.gRC and after 48h cells were transfected with the  
981 Cas9-GFP protein and differentiated into mature RBCs following a 21 days differentiation protocol.  
982 **(B)** Correlation between VCN and InDel frequency in cells treated with LV AS3m.C (2 mobilized  
983 SCD donors).  $R^2$  and line-of-best-fit equation are indicated. **(C)** InDel frequency in LV AS3m.C-  
984 treated SCD HSPCs measured by TIDE analysis after PCR amplification and Sanger sequencing of  
985 the target region in *HBB* exon 1 and the potential off target region in the transgene (AS3m). **(D)**

986 Evaluation of off-target activity. GUIDE-seq analysis of gR-C in 293T cells (left panel). The  
987 protospacer targeted by gR-C and the PAM are shown in the first line. Off-targets and their  
988 mismatches with the on-target (highlighted in color), sequencing read counts and chromosomal  
989 position are reported. Deep-sequencing analysis of off-target editing events in mature erythroblasts  
990 derived from SCD HSPCs treated with LV AS3m.C (right panel). Transduced and mock transfected  
991 SCD cells (Ctr) are indicated in red and edited samples (AS3m.C) in black. **(E)** Correlation between  
992 VCN (left panel) or Indel frequency (right panel) and percentage of HbS and HbAS3 (determined  
993 by CE-HPLC) in SCD RBCs derived from mock-transfected (orange and light blue) and Cas9-  
994 transfected (red and dark blue) SCD HSPCs transduced with LV AS3m.C (2 mobilized SCD  
995 donors).  $R^2$  and line-of-best-fit equation are indicated. Dashed lines indicate the VCN required to  
996 achieve equal amounts of HbS and HbAS3. **(F)** Relative expression of *HBB* mRNA normalized to  
997  $\alpha$ -globin in untreated SCD cells (Ctr) (n=6) and in cells treated with LV AS3m.C (n=8; 2 mobilized  
998 SCD donors). \*\*\*\* p < 0.0001 (unpaired t-test). Horizontal lines indicate median and first and third  
999 quartiles. **(G)** Representative CE-HPLC chromatograms showing the Hb profile of *in vitro*  
1000 differentiated mature erythroblasts. From top to bottom:  $\beta$ -thalassemic cells (thal), healthy donor  
1001 cells (HD), HD cells treated with gR-C plasmid (HD+gR-C), SCD cells (SCD), SCD cells  
1002 transduced with LV AS3m.C and mock-transfected, SCD cells transduced with LV AS3m.C and  
1003 transfected with Cas9-GFP protein.

1004

1005 **Figure 4: Testing of LV AS3m.13bpdel and LV AS3m.BCL11A in SCD HSPCs.**

1006 **(A)** Schematic representation of the protocol used to transduce and transfect SCD HSPCs. 24h after  
1007 thawing, HSPCs were transduced with LV AS3m13bpdel and LV AS3m.BCL11A and after 48h  
1008 cells were transfected with the Cas9-GFP protein and differentiated into mature RBCs following a  
1009 21 days differentiation protocol. **(B)** Correlation between VCN and InDel frequency in cells treated  
1010 with LVs AS3m.BCL11A (1 mobilized SCD donor) and AS3m.13bpdel (2 mobilized SCD donors).  
1011  $R^2$  and line-of-best-fit equation are indicated. **(C)** Deep-sequencing analyses of the 13bpdel off-

1012 target in mature erythroblasts derived from adult SCD HSPCs treated with LV AS3m.13bpdel.  
1013 Transduced and mock transfected SCD cells (Ctr) are indicated in red and edited samples  
1014 (AS3m.13bpdel) in black. **(D)** GUIDE-seq analysis of gR-BCL11A in 293T cells. The protospacer  
1015 targeted by gR-BCL11A and the PAM are shown in the first line. Off-targets and their mismatches  
1016 with the on-target (highlighted in color), sequencing read counts and chromosomal position are  
1017 reported. **(E)** Relative expression of *HBG* mRNA normalized to  $\alpha$ -globin in untreated SCD cells  
1018 (Ctr) (n=5) and cells treated with LV AS3m.13bpdel (n=14, 2 SCD donors). \*\*\*  $p < 0.001$   
1019 (unpaired t-test). Horizontal lines indicate median and first and third quartiles. **(F)** Representative  
1020 flow cytometry analysis of F-cells in RBCs derived from untreated (Ctr UT; light blue), and LV  
1021 AS3m.13bpdel-treated SCD HSPCs mock-transfected (medium blue) or transfected with Cas9-GFP  
1022 (dark blue) (2 mobilized SCD donors). **(G)** Correlation between VCN and percentage of HbS and  
1023 HbAS3 (determined by CE-HPLC) in cells derived from mock-transfected (orange and light blue)  
1024 and Cas9-transfected (red and dark blue) SCD HSPCs transduced with LV AS3m.13bpdel (2  
1025 mobilized SCD donors). We plotted the percentage of HbS or HbAS3+HbF over the total Hbs.  $R^2$   
1026 and line-of-best-fit equation are indicated. Dashed lines indicate the VCN required to achieve equal  
1027 amounts of HbS and HbAS3. **(H)** Correlation between Indel frequency and percentage of HbS and  
1028 HbAS3 (determined by CE-HPLC) in cells derived from Cas9-transfected SCD HSPCs transduced  
1029 with LV AS3m.13bpdel (2 mobilized SCD donors).  $R^2$  and line-of-best-fit equation are indicated.

1030

1031 **Figure 5: The bifunctional LVs AS3m.C and AS3m.13bpdel reduce RBC sickling**

1032 *In vitro* sickling assay measuring the proportion of sickled RBCs under hypoxic conditions (0%  
1033 O<sub>2</sub>). We reported the percentage of sickling RBCs (left panel) and representative photomicrographs  
1034 of RBCs derived from control (Ctr), LVs AS3m.C and AS3m.13bpdel samples that were either  
1035 mock-transfected or transfected with Cas9-GFP (right panel; 2 SCD donors). Arrows indicate  
1036 sickling cells. Data are expressed as mean $\pm$ SEM. Scale bar, 20  $\mu$ m (upper left).

1037

1038 **Figure 6: The bifunctional LV down-regulating HbS does not generate a  $\beta$ -thalassemic**  
1039 **phenotype**

1040 (A) Schematic representation of the protocol used to evaluate erythroid differentiation and RBC  
1041 parameters. We transduced SCD/HD HSPCs with LV AS3m.C and transfected them with Cas9  
1042 protein. As controls, we transfected SCD/HD HSPCs with RNPs containing gR-C. Pictures of *in*  
1043 *vitro* cultured RBCs were taken using the Phasics SID4-HR GE camera. The BIO-Data interface  
1044 software was used to analyze RBC images. (B) CE-HPLC quantification of Hb tetramers in  
1045 untreated HD and SCD cells (Ctr UT), gR-C-treated HD and SCD cells (gR-C) and LV AS3m.C-  
1046 treated SCD HSPCs that were mock-transfected (“-“) or transfected with Cas9-GFP protein. We  
1047 plotted the percentage of each Hb type over the total Hb tetramers. VCN are reported in blue and  
1048 InDels in black below the graph. The  $\alpha$ -non- $\alpha$ -globin ratio (determined by RP-HPLC) is reported  
1049 on top of the histograms.

1050

1051 **Figure 7: Erythroid differentiation and RBC parameters were not impaired in cells derived**  
1052 **from LV AS3m.C-transduced, edited SCD HSPCs.**

1053 (A-E) Flow cytometry analysis of the enucleation rate and of the early (CD71, CD36 and CD49d)  
1054 and late (CD235A and Band3) erythroid markers at day 13, 16 and 19 or 20 of erythroid  
1055 differentiation of untreated HD (n=1) and SCD (n=3) cells (Ctr UT), gR-C-treated HD (n=1) and  
1056 SCD (n=1) cells (gR-C) and LV AS3m.C-treated SCD HSPCs that were mock-transfected or  
1057 transfected with Cas9-GFP protein (n=3). VCN and InDels values are reported below the graph as  
1058 mean $\pm$ SEM. (A) Enucleation rate measured using DRAQ5 nuclear staining. (B-D) Proportion of  
1059 CD71<sup>+</sup>, CD36<sup>+</sup> and CD235A<sup>+</sup> cells during erythroid differentiation. (E) Expression of CD49d and  
1060 Band3 during the erythroid differentiation. During terminal erythroid differentiation, cells lose  
1061 CD49d expression. (F-I) RBC parameters extracted using the BIO-Data software. RBCs were  
1062 obtained after 19 days of differentiation from SCD HSPCs transduced with LV AS3m.C and either  
1063 mock- or Cas9-transfected. As controls, we used RBCs obtained from SCD/HD HSPCs transfected

1064 with RNPs containing gR-C For each population, data were normalized to the total number of  
1065 RBCs, and are reported as overlaid histograms. Darker colors represent controls and lighter colors  
1066 edited samples. From top to bottom: control HD RBCs compared with HD RBCs derived from  
1067 HSPCs treated with gR-C; control SCD RBCs compared with SCD RBCs derived from HSPCs  
1068 treated with gR-C; control SCD RBCs derived from HSPCs transduced with LV AS3m.C and  
1069 mock-transfected compared to RBCs derived from HSPCs transduced with LV AS3m.C and  
1070 transfected with Cas9 protein. **(F)** Dry mass (pg). **(G)** Surface ( $\mu\text{m}^2$ ). **(H)** Perimeter ( $\mu\text{m}$ ). **(I)**  
1071 Ellipticity.

1072

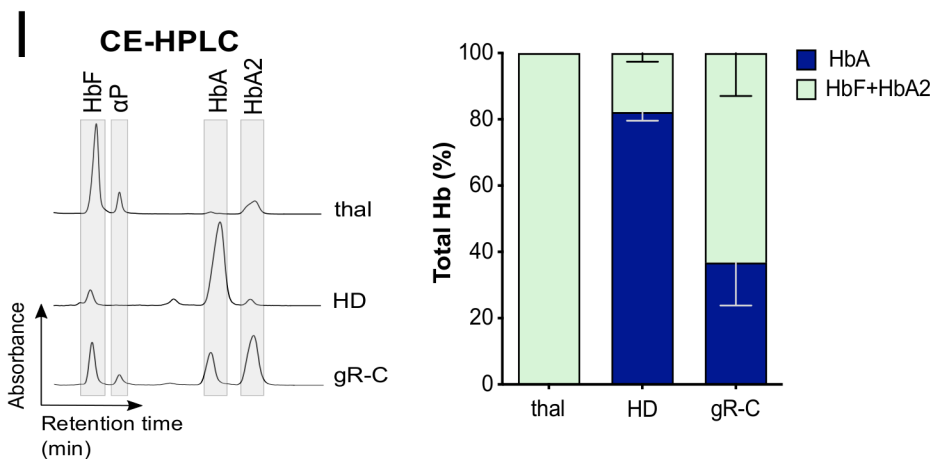
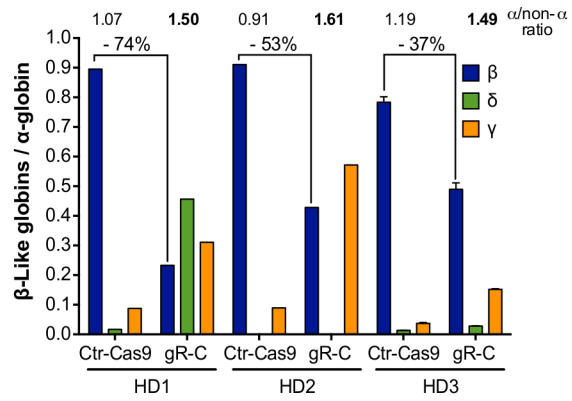
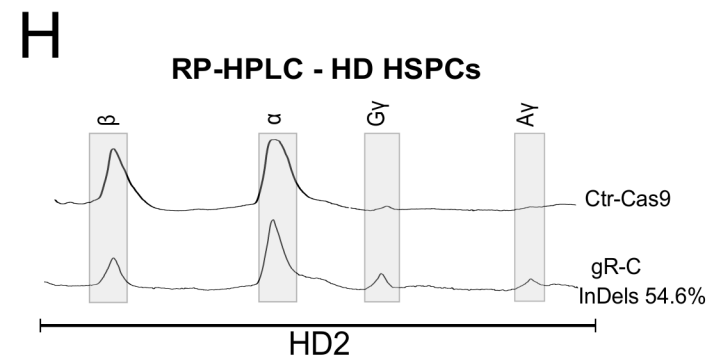
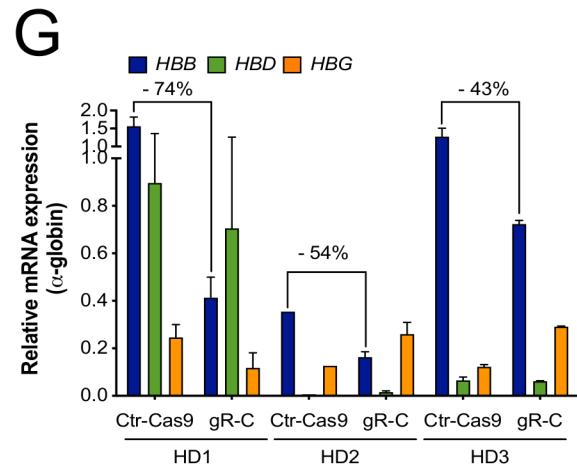
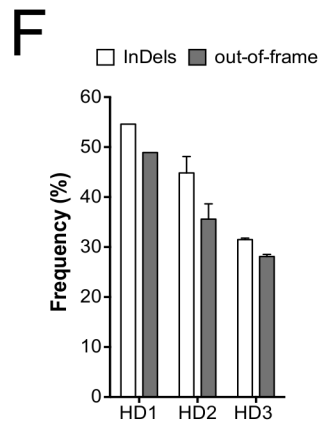
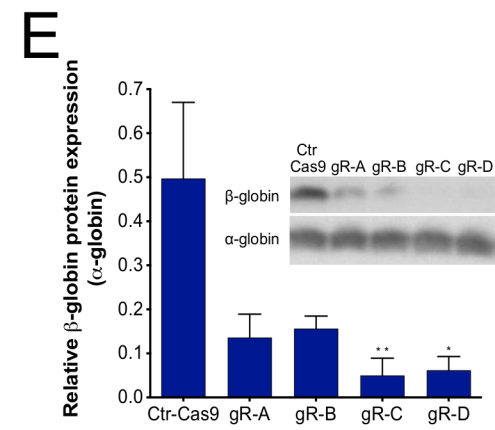
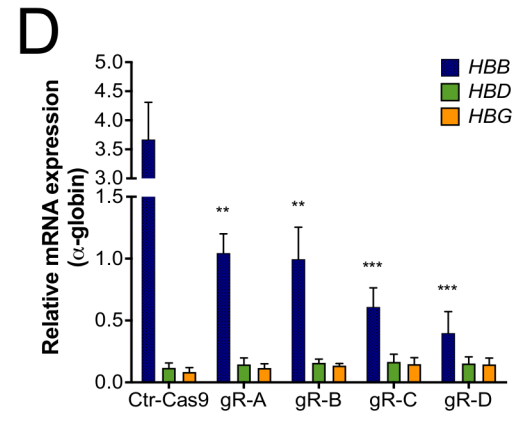
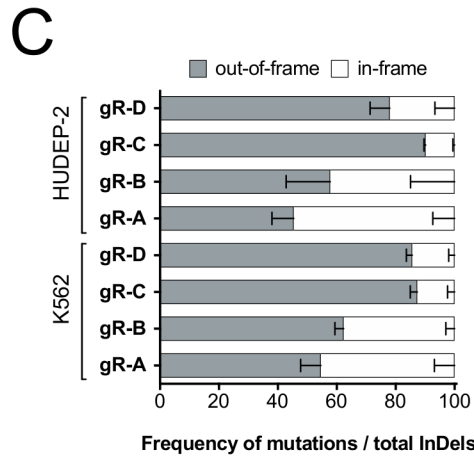
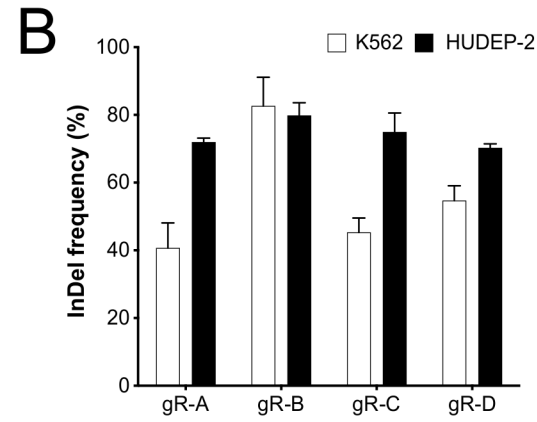
1073

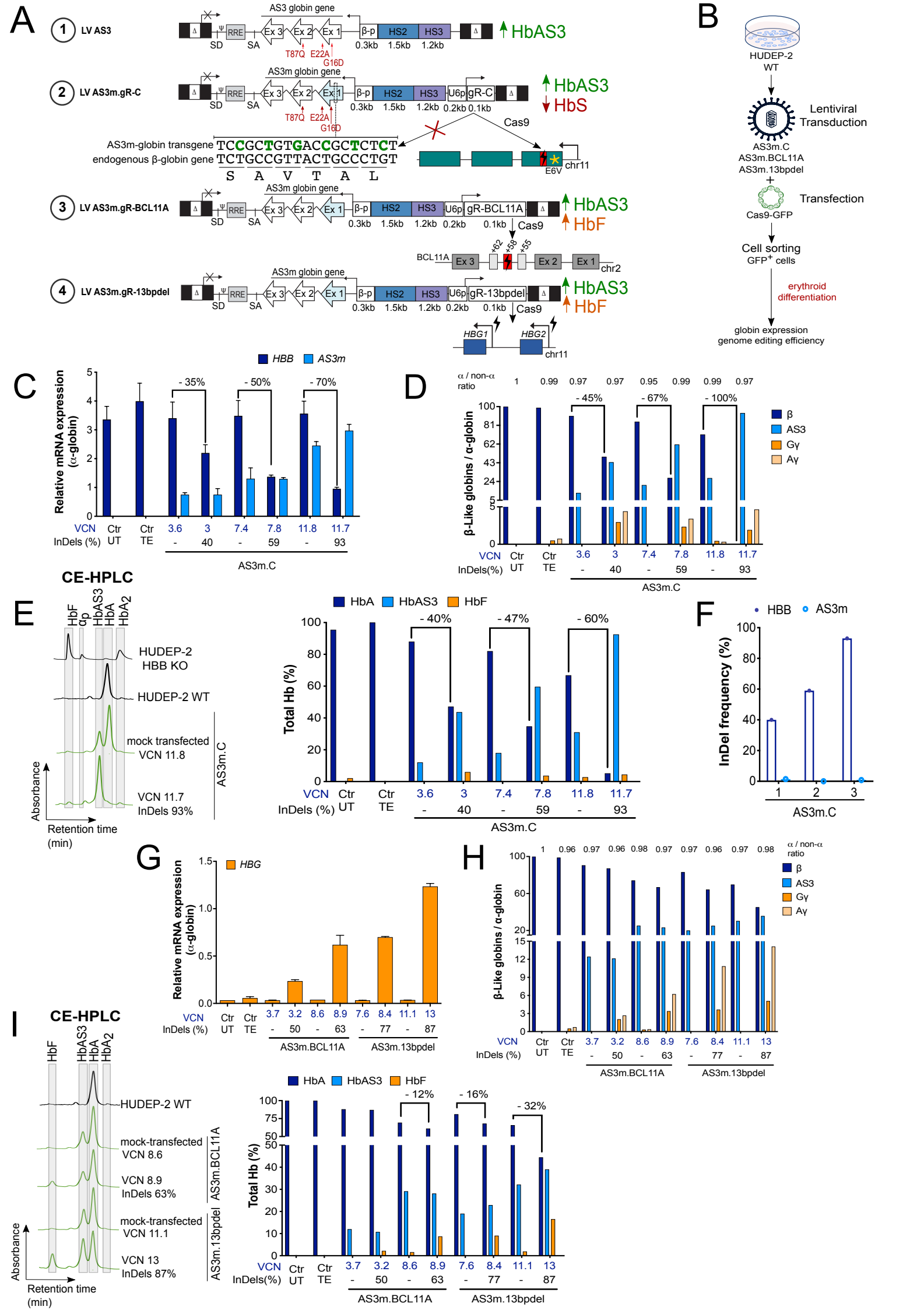
**A**

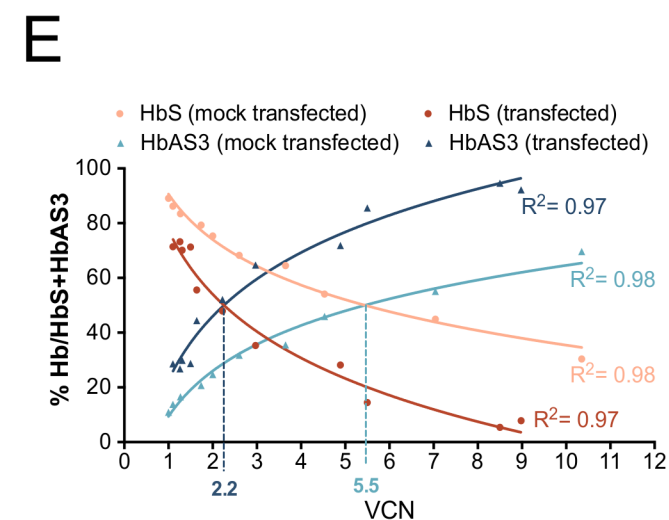
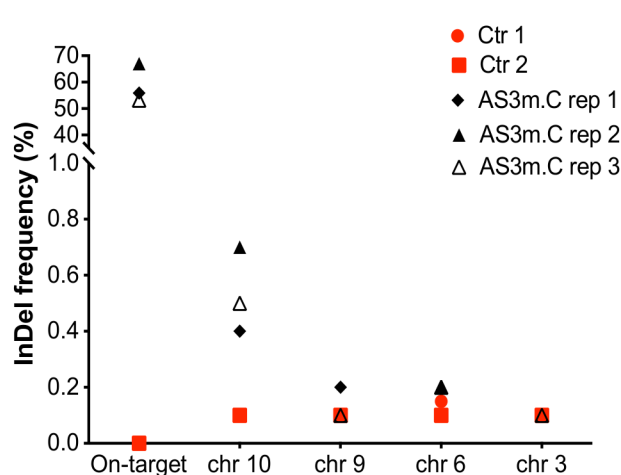
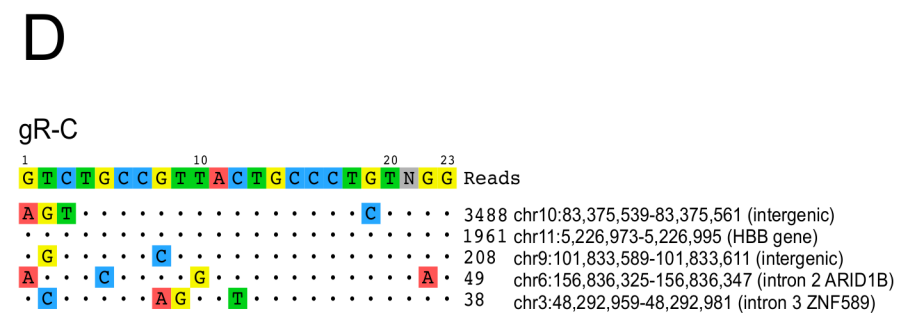
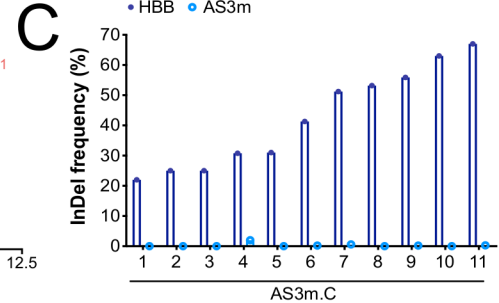
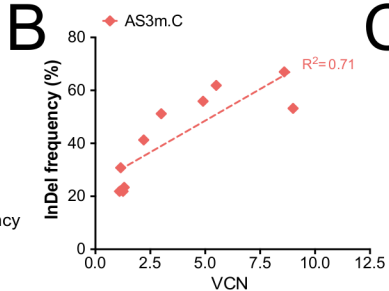
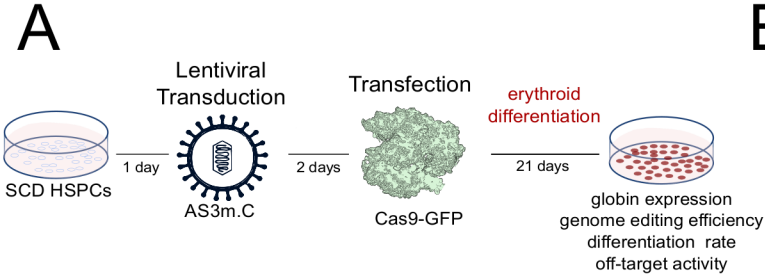
gR-A  
gR-B  
gR-C  
gR-D

GAGGAGAAGTCTGCCGTTAC  
TCTGCCGTTACTGCCCTGT  
AAGGTGAACGTGGATGAAGT

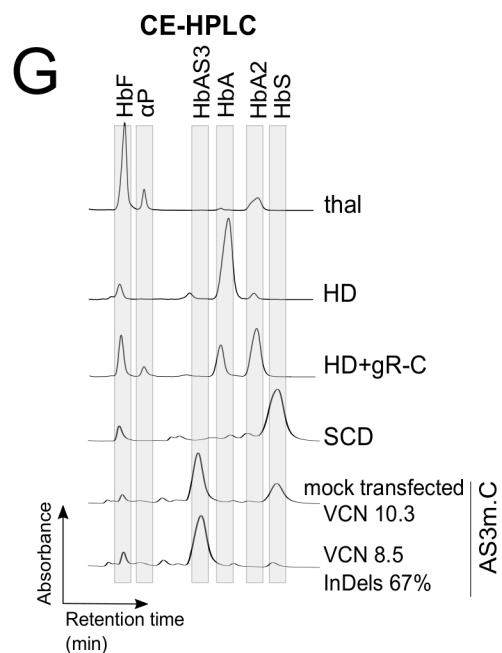
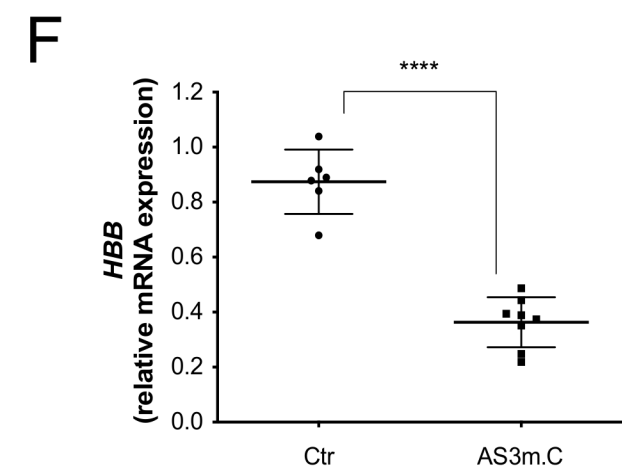
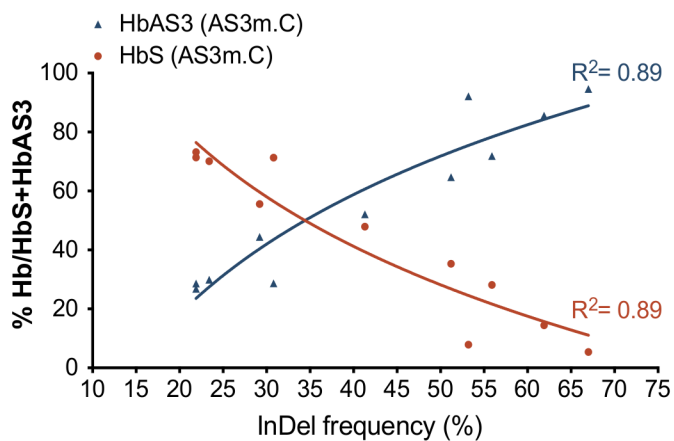
*HBB* exon 1 CTGACTCCTGAGGAGAAGTCTGCCGTTACTGCCCTGTGGGGCAAGGTGAACGTGGATGAAGTTGG

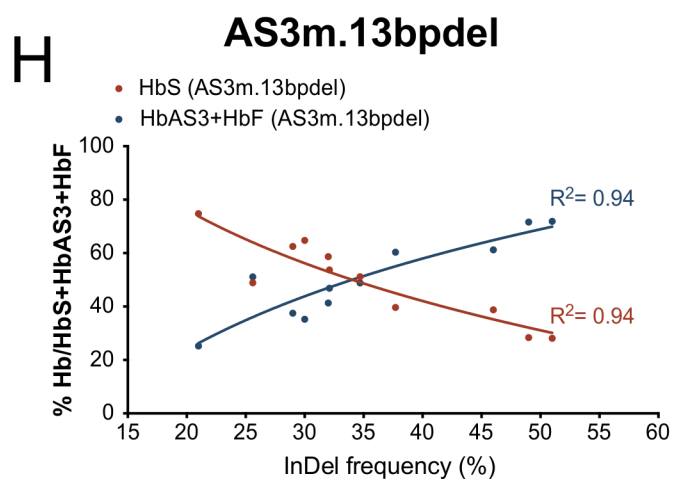
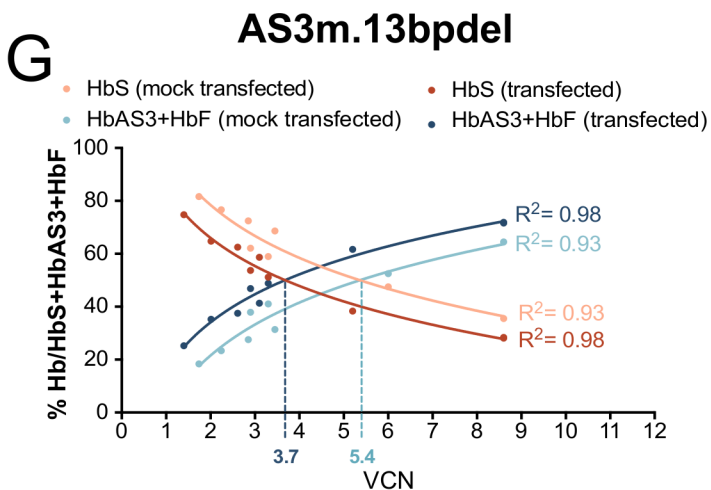
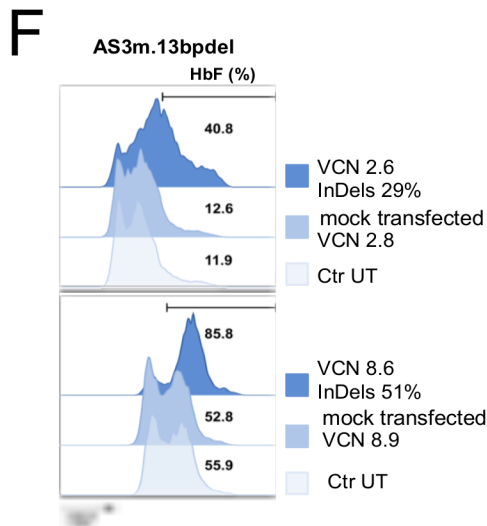
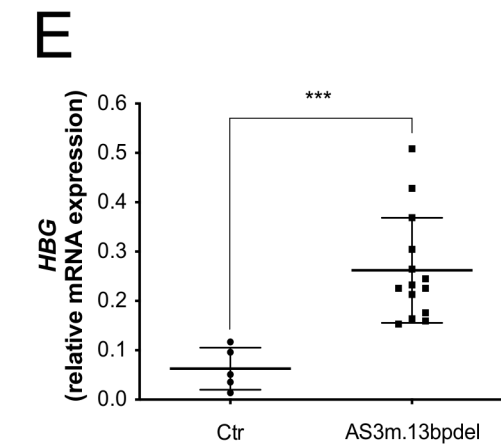
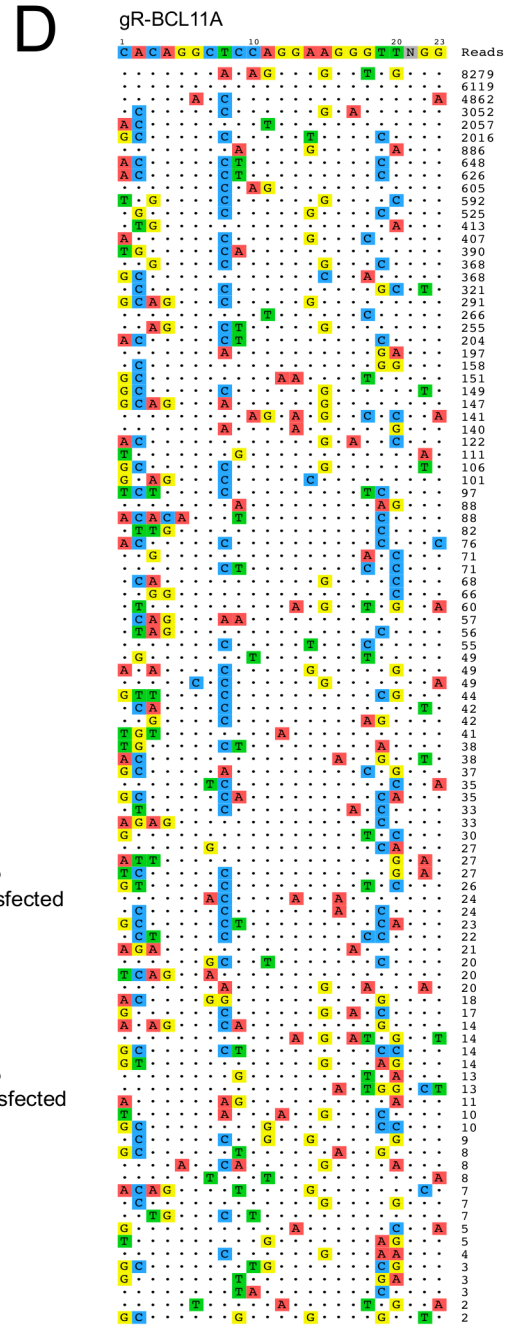
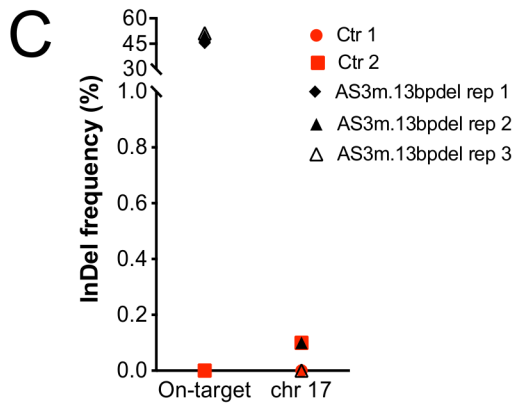
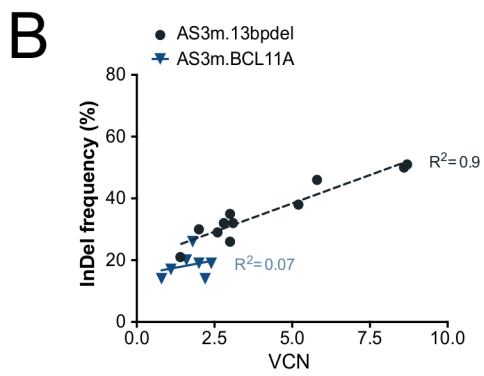
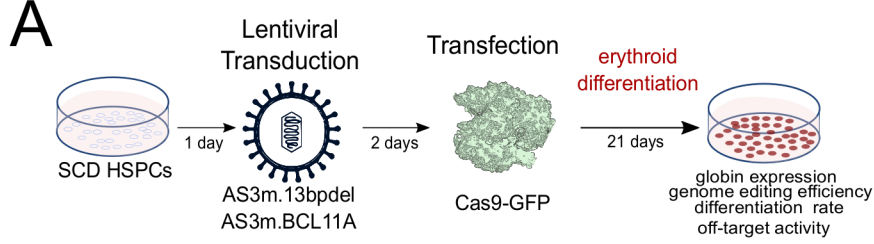


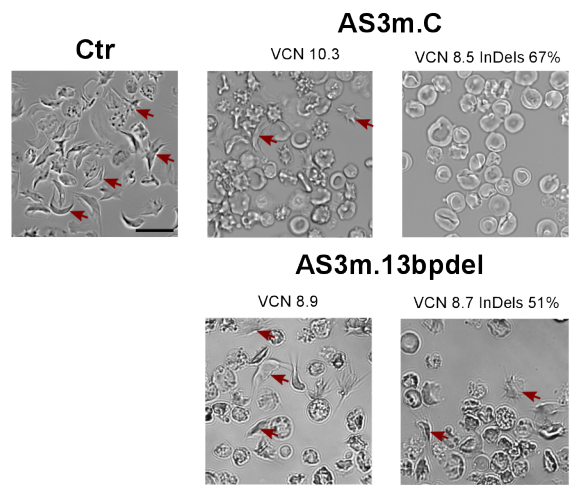
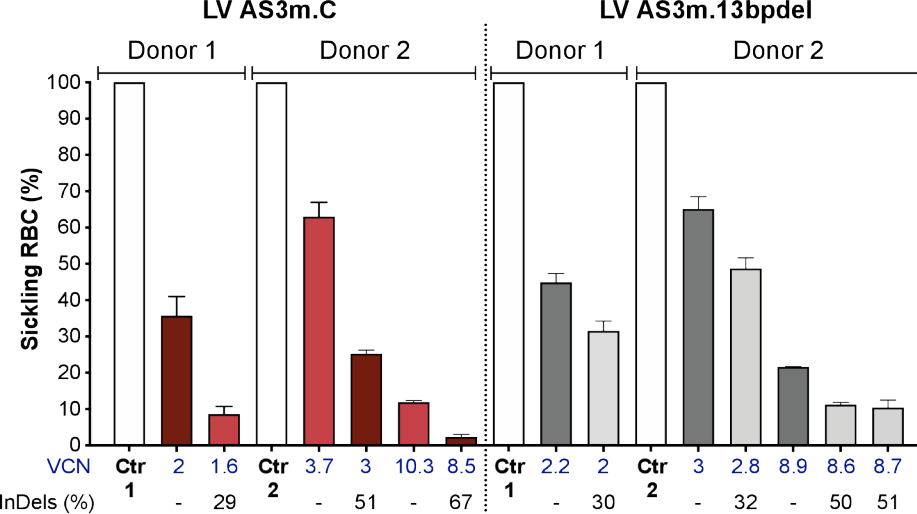


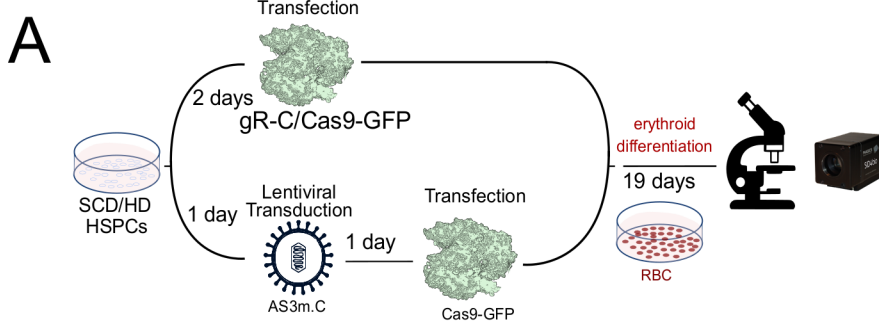


**AS3m.C**

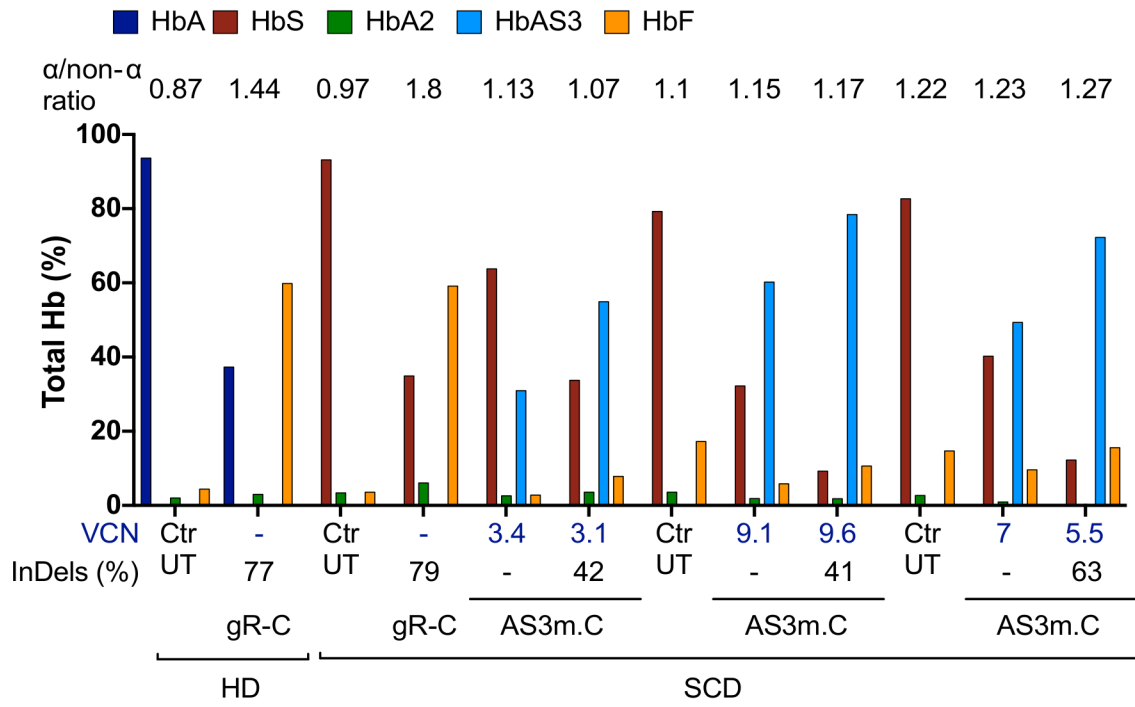


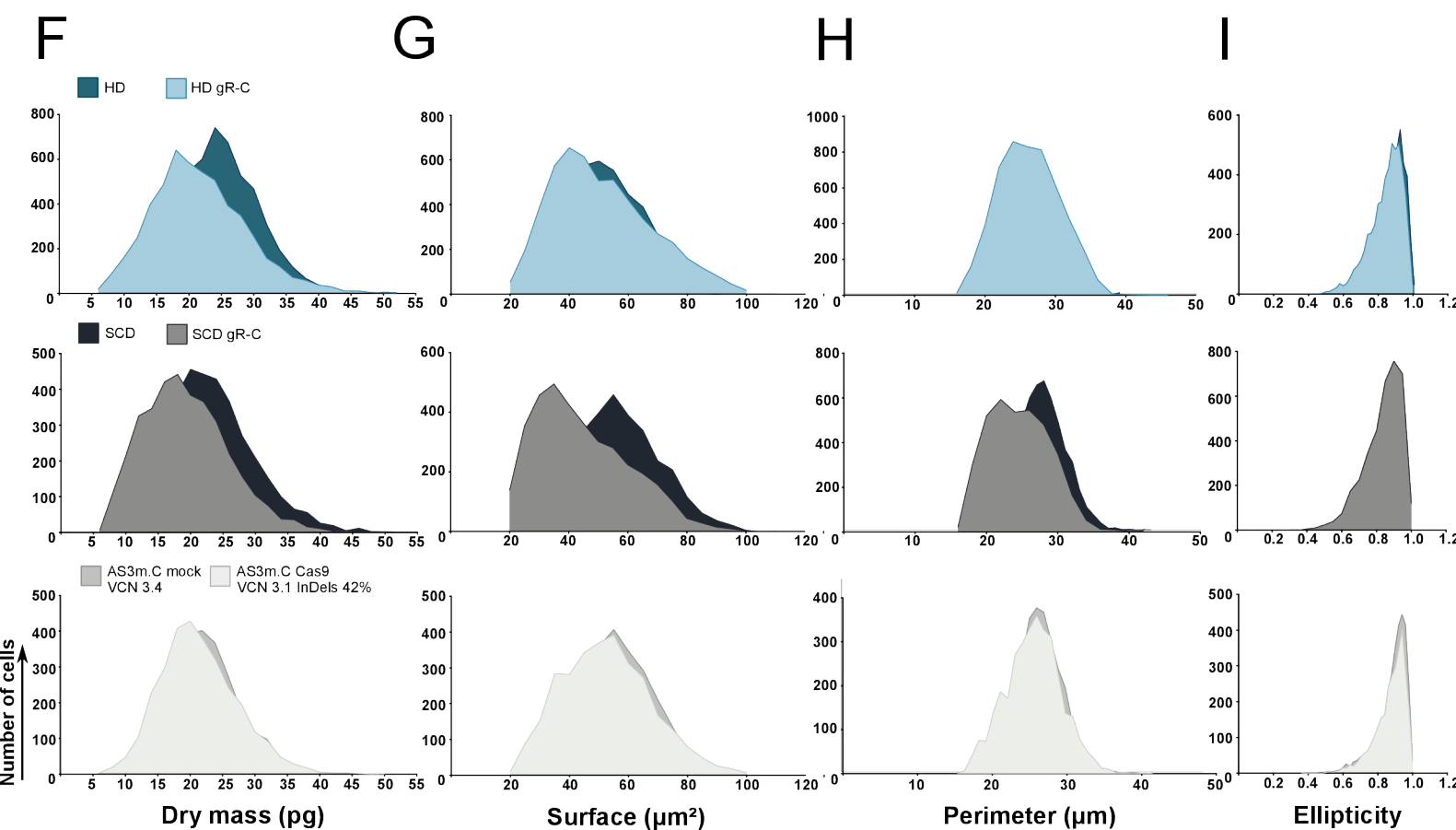
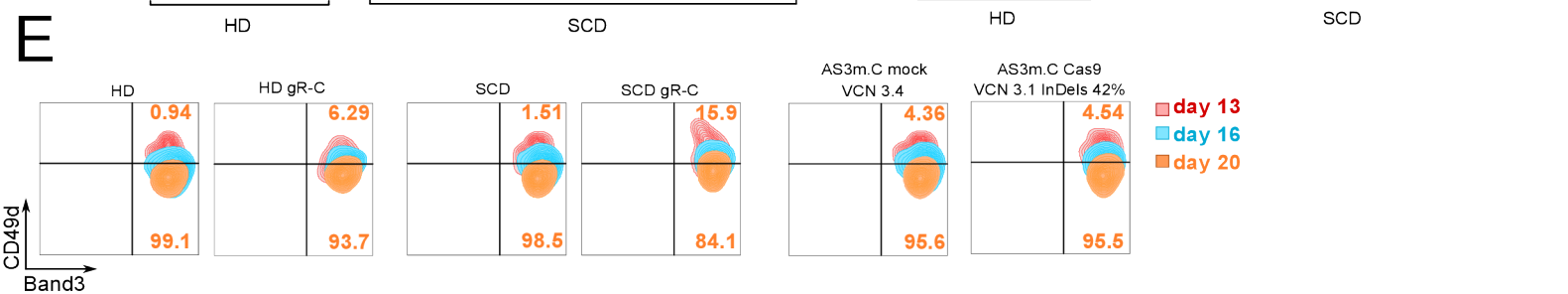
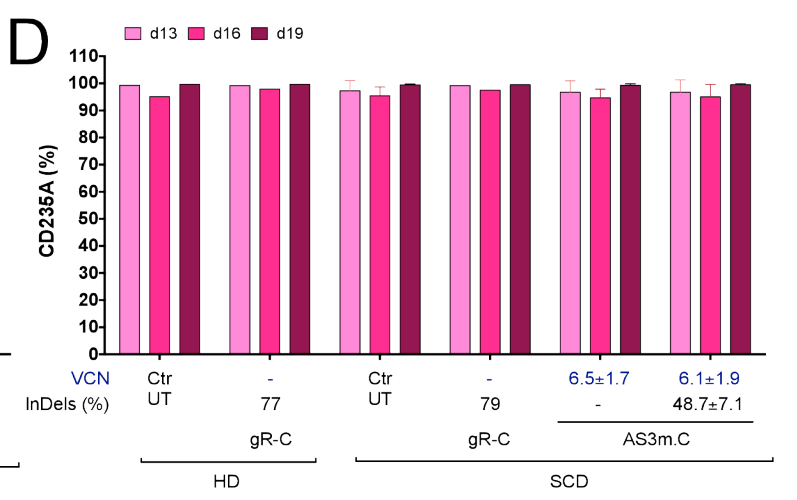
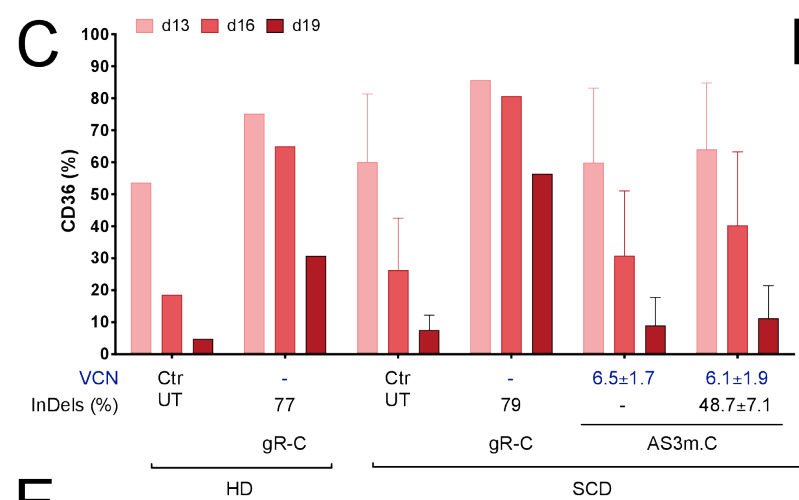
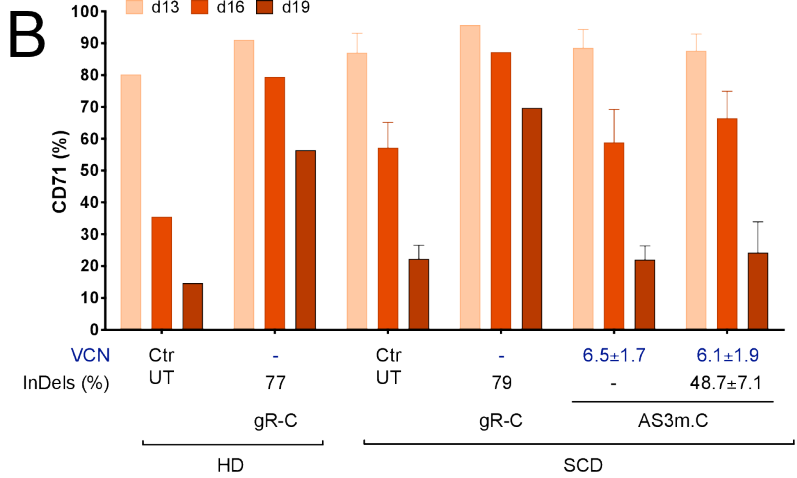
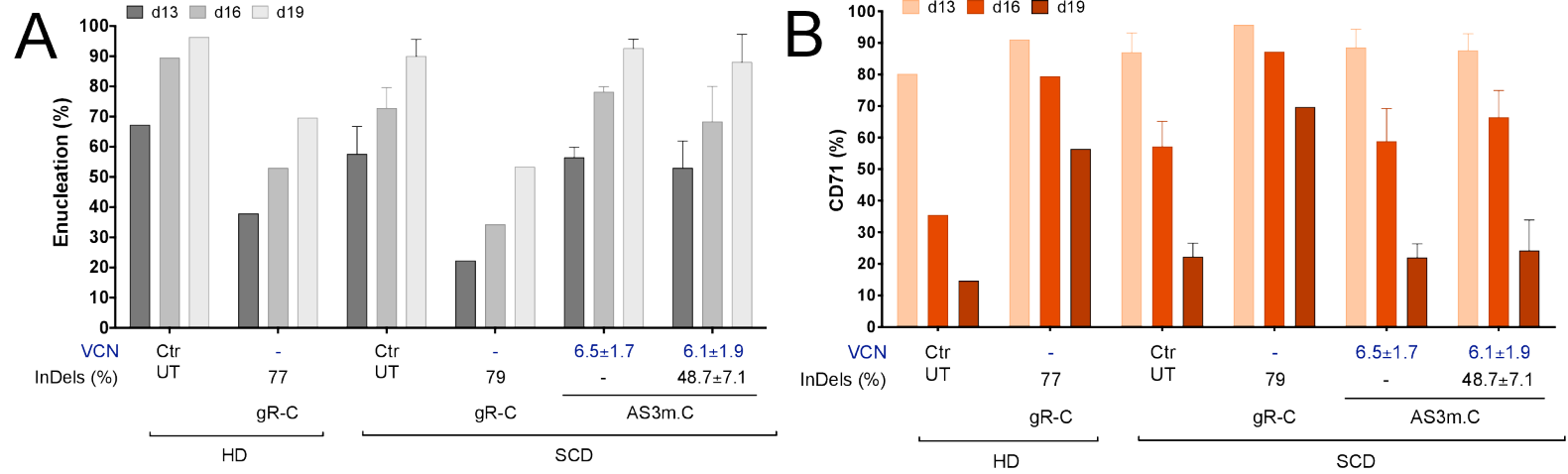






**B**





 Sick cell disease (SCD) patient red blood cell (RBC) (normoxia)

 SCD patient RBC (hypoxia)

 AS3-containing RBC

 AS3-containing RBC with decreased HbS levels

 AS3-containing RBC with increased HbF levels

